



Aalborg Universitet

AALBORG UNIVERSITY
DENMARK

Performance and control strategy development of a PCM enhanced ventilated window system by a combined experimental and numerical study

Hu, Yue; Guo, Rui; Heiselberg, Per Kvols

Published in:
Renewable Energy

DOI (link to publication from Publisher):
[10.1016/j.renene.2020.03.137](https://doi.org/10.1016/j.renene.2020.03.137)

Creative Commons License
CC BY-NC-ND 4.0

Publication date:
2020

Document Version
Publisher's PDF, also known as Version of record

[Link to publication from Aalborg University](#)

Citation for published version (APA):

Hu, Y., Guo, R., & Heiselberg, P. K. (2020). Performance and control strategy development of a PCM enhanced ventilated window system by a combined experimental and numerical study. *Renewable Energy*, 155(August 2020), 134-152. <https://doi.org/10.1016/j.renene.2020.03.137>

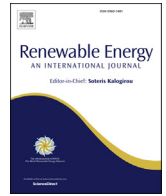
General rights

Copyright and moral rights for the publications made accessible in the public portal are retained by the authors and/or other copyright owners and it is a condition of accessing publications that users recognise and abide by the legal requirements associated with these rights.

- Users may download and print one copy of any publication from the public portal for the purpose of private study or research.
- You may not further distribute the material or use it for any profit-making activity or commercial gain
- You may freely distribute the URL identifying the publication in the public portal -

Take down policy

If you believe that this document breaches copyright please contact us at vbn@aub.aau.dk providing details, and we will remove access to the work immediately and investigate your claim.



Performance and control strategy development of a PCM enhanced ventilated window system by a combined experimental and numerical study

Yue Hu^{*}, Rui Guo, Per Kvols Heiselberg

Aalborg University, Division of Architectural Engineering, Department of Civil Engineering, Thomas Manns Vej 23, DK-9220, Aalborg Øst, Denmark

ARTICLE INFO

Article history:

Received 10 December 2019

Received in revised form

29 February 2020

Accepted 23 March 2020

Available online 27 March 2020

Keywords:

Phase change material

Ventilated window

Ventilation preheating/precooling

Control strategy

Building energy efficiency

ABSTRACT

This study proposes a PCM enhanced ventilated window (PCM-VW) system for ventilation preheating/precooling purposes for building energy conservation. It is designed into a summer night cooling application and a winter solar energy storage application using different control strategies. An EnergyPlus model of the PCM-VW is built to investigate the control strategies. Next, a full-scale experiment is conducted to study the working principle of the PCM-VW and to validate the model. With the validated model, the thermal and energy performance of the PCM-VW is compared to 2 other ventilation systems and shows that the PCM-VW can greatly decrease the cooling/heating energy demand for both summer and winter applications. Finally, the paper proposes control strategies for residential applications under Danish climate conditions. The developed control strategy for summer night cooling application is to use between-glass reflection shading, ventilate directly from PCM heat exchanger to the room while applying VW self-cooling for ventilation pre-cooling mode, and heat the room with air from VW to prevent overcooling of the room. The developed control strategy for winter solar energy storage application is to use between-glass absorption blind, make use of the hot air in VW, and to cool the VW by self-cooling and bypass ventilation to prevent overheating of the room. With the developed control strategies, the building energy saving is up to 62.3% and 9.4% compared to the primitive summer and winter control strategies respectively.

© 2020 The Authors. Published by Elsevier Ltd. This is an open access article under the CC BY-NC-ND license (<http://creativecommons.org/licenses/by-nc-nd/4.0/>).

1. Introduction

Many researchers and engineers have successfully applied phase change material (PCM) in building components as latent heat thermal energy storage (LHTES) systems [1]. Compared to sensible heat storage systems that change the storage material temperature, LHTES systems need a much smaller volume of material to store the same amount of energy. The latent heat storage systems, especially PCMs, have recently drawn much attention in the research area and the market, due to their high heat storage ability [2].

The application of PCM in buildings can be divided into passive and active systems. The passive systems with PCMs for building applications include PCMs in the wallboard [3–7], roof [8], concrete system [9–11], glazing [12,13], shading [14], and furniture [15,16]. Those passive systems have a slow response to the heating and

cooling needs and are usually used as auxiliaries for the building environment. The active systems with PCMs involve water, air, or other media to accelerate the heat charge and discharge processes of PCMs. These systems have a shorter response time and contribute to a better heat transfer coefficient by replacing the free convection by forced convection. Active PCM systems include PCMs in the ceiling [17], floor [18,19], double-skin façade [20], ventilated window [21], domestic hot water systems [22], and HVAC system [23]. The systems are used for building heating or cooling purposes, usually operating in combination with ventilation or water system.

Building energy systems can benefit from the PCM application when adopting renewable energy as heat or cold sources. The stored energy can be used to create a good indoor environmental quality and save the building energy. One of the most common renewable energies for TES is solar energy. Solar energy has to be stored as it is highly dependent on the outdoor climate conditions during the daytime. PCM has been used as the storage medium in most of the cases, due to its high energy storage ability. The conventional PCM solar energy system includes a PCM tank, a solar

^{*} Corresponding author.

E-mail address: hy@civil.aau.dk (Y. Hu).

collector, and some heat transfer fluid between the solar collector and the PCM tank [24,25]. PCM can be used as the heat transfer fluid as well [26].

Windows account for a large part of the total building heating and cooling load, regardless of adopting coatings, sealed glazing, and tight gaskets [27]. The basic concept of the ventilated window (VW) is to control the outdoor airflow passing through the cavity of the double window. The aim of the VW is to decrease solar heat gain through the window in summer and minimize the room heating load and improve thermal comfort by utilizing the solar radiation to preheat the ventilation air in winter [28]. Several experimental and numerical research have investigated the VW performance [29–35]. It is found out that the VW can decrease cooling and/or heating demand and improve indoor thermal comfort. However, the pretreated supply air temperature could not reach the room air temperature [35]. Therefore, the supply air temperature needs to be further heated or cooled by additional means. PCM can be a good candidate to provide additional thermal storage in the VW to form an active system for better performance of the VW. In the summer night the PCM is cooled down by night ventilation. It cools the ventilation air in the daytime to decrease the room's cooling load. While in winter, it stores the solar energy in the daytime and heats up the air when heating demand is present.

Few studies have investigated the combination of the VW and PCM. In previous works, the authors demonstrated that a PCM heat exchanger can cool down the ventilated air 6.5 °C average and save 3.19 MJ energy per day based on a night ventilation experiment in summer. The depth of PCM plates was also optimized based on the numerical model, which can reduce the material cost by 16.9% in Copenhagen, Denmark [21]. The authors also investigated the ability of PCMVW pre-cooling in summer and pre-heating in winter through full-scale experiments in Aalborg, Denmark [36]. However, whether the ventilation control strategy of PCMVW adopted in previous work is the best remains to be answered. Moreover, the cooling potential of the PCMVW in previous works was not high enough, which may need extra elements to be added for improvement. In this paper, the performance of the PCMVW is examined by comparing it with two other ventilation systems. In addition, the control strategies for summer and winter applications are developed respectively with the adding of blinds control to further enhance the energy-saving potential of the PCMVW.

Therefore, this paper investigates the ventilation control strategy of the PCMVW through an EnergyPlus model for a 3-rooms apartment with PCMVWs under Danish climate conditions. Later on, the paper introduces a full-scale experiment in the façade lab of Aalborg University to investigate the thermal properties of the PCMVW. The experiment is done in 3 parts: night cooling application, solar energy storage application and blinds for advanced VW control. The simulation results are compared with the experimental data. In addition, the PCMVW is compared to 2 other ventilation systems in regards to the thermal and energy performance. Lastly, the model is used for control strategy development for summer night cooling application and winter solar energy storage application respectively.

2. Model description

The apartment investigated is a part of a nearly zero-energy residential building with high air tightness and low U value for the constructions. It is a 3-rooms apartment on the second floor of a 3-floor residential building. Fig. 1 shows the plan view of the Danish demonstration site and the floor plan of the apartment; rooms are simulated as separate thermal zones, including four windows in total. Only the southwest and northeast walls are set as external

walls. Other walls are internal walls adjacent to internal thermal zones. Table 1 shows the properties of the external walls. The infiltration rate is set as 0.1 h⁻¹. The heating set point of the room is 22 °C, and the cooling set point is 26 °C, by the ideal load HVAC system. An exhaust fan with 300 Pa pressure rise and total efficiency of 0.7 drives and controls the outdoor air into the indoor room through the heat exchanger and double glazing window. The specific fan power of the fan fulfills the recommended “good-practice” from the technical note AIVC 65 [37]. The daytime ventilation airflow rate should be larger than the minimum requirement of the fresh air per person or per floor area but should be within the thermal comfort range so it does not cause draft to the indoor environment. The ventilation flow rate is 30 m³/h/person for all the three models.

The PCMVW model is separated into three thermal zones: the room, the ventilated window (VW), and the PCM heat exchanger, as seen in Fig. 2. The VW is made by a double-glazing panel on the outer surface, a single glazing panel on the inner side, and a ventilated cavity in between them. The glass for both the double-glazing and single glazing is 6 mm. A 13 mm air gap is in the double glazing panel. Parallel PCM plates compose the PCM heat exchanger. The thickness of the plates is 12.5 mm and the air gap between two plates is 5 mm, which is based on the configuration optimization in Ref. [21,38]. The thin PCM plates and relatively large surface area make it faster to activate the PCM heat exchanger. The inlet of the PCM heat exchanger is at the bottom of it. The outlet of the PCM heat exchanger is connected to the ventilated window. The outlet of the ventilated window is either to the indoor room or to the outside environment. The between-glass internal shading is made by venetian blinds with absorption coating (solar reflectance coefficient = 0.15) on one surface and reflection coating (solar reflectance coefficient = 0.6) on the other side. The absorption side is turned on towards outdoor for winter solar storage application, while the reflection side is turned on towards outdoor for summer cooling application.

The Conduction Finite Difference (CondFD) heat balance algorithm is used in EnergyPlus. It complements the conduction transfer function (CTF) algorithm when simulating the phase change material or materials with changeable thermal conductivities. The zone time step using the CondFD algorithm can be much shorter than CTF. The algorithm uses a fully implicit scheme to solve the heat transfer equations. The enthalpy as a function of the temperature of the PCM is set as the input of the model. The heat capacity of the PCM is calculated based on Equation (1).

$$Cp(T) = \frac{H_i^j - H_i^{j-1}}{T_i^j - T_i^{j-1}} \quad (1)$$

For PCM with hysteresis, the heat capacity depends not only on the current state but also on the previous state. It presents the hysteresis effect between the freezing process and the melting process.

$$Cp(T) = f(T_i^j, T_i^{prev}, PhaseState_j, PhaseState_{prev}) \quad (2)$$

The PCM in the heat exchanger part is a mixture of fiber (50%) and paraffin wax (50%). The heat capacity of the compound was measured by differential scanning calorimetry (DSC) technology in previous work [21]. Fig. 3 shows the inputs of the PCM heat capacity in EnergyPlus.

The internal loads include the people load and the electricity load. The number of the person for the whole apartment is 1.72 and the people load is 90 W/person, which is based on the surveys for apartments in Denmark in Ref. [39]. The occupant schedule and the

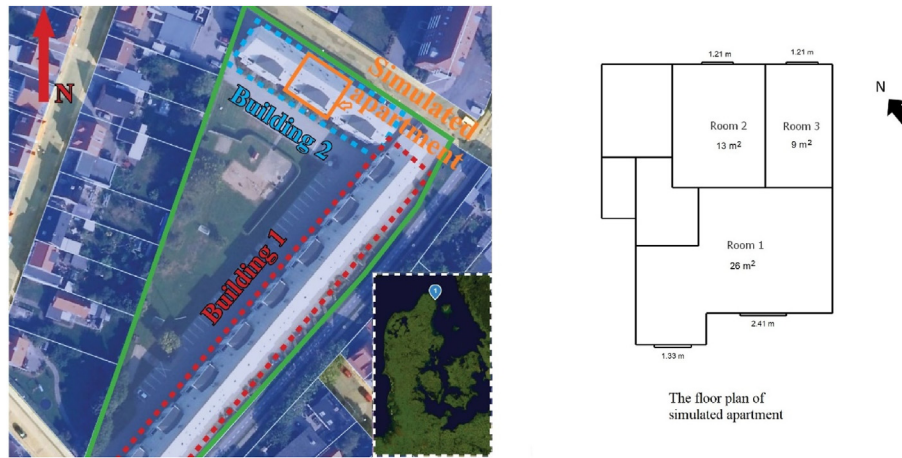


Fig. 1. Plan view of the Danish demonstration site and the apartment used for the investigation.

Table 1
The properties of the external wall.

Material	Thickness [m]	Thermal Conductivity [W/m·K]	Resistance [m²·K/W]
Wood	0.02	0.12	0.13
Insulation	0.25	0.04	6.62
Brick	0.31	0.77	0.40

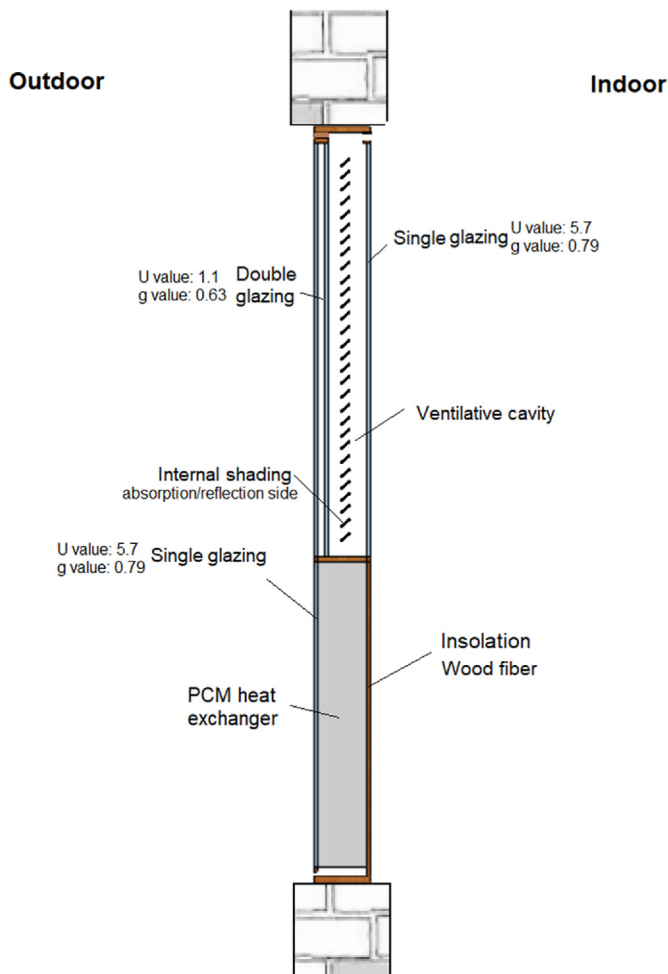


Fig. 2. The overview of the VW + PCM model.

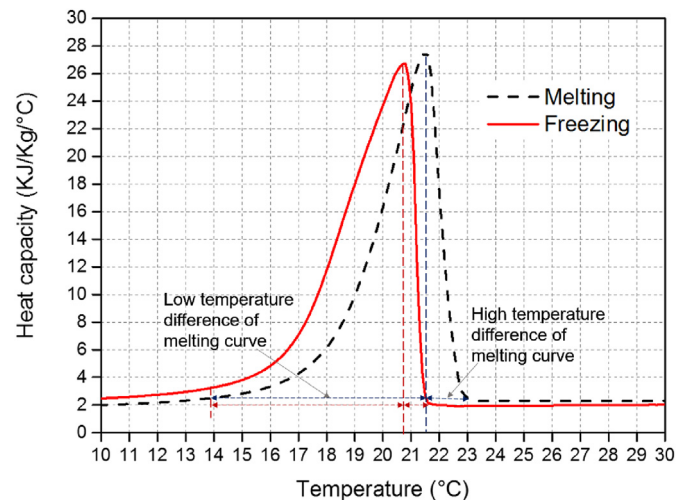


Fig. 3. The heat capacity of the PCM measured by DSC [21].

electricity schedule are shown in Fig. 4 and Fig. 5 based on the survey in the report [40]. The people load is more in the evenings and differs between weekdays and weekends. The electricity load is also diverse between weekdays and weekends and differs among the months. The electricity load at a full percentage (100%) is 592.18 W. The people load and the electricity load are evenly distributed in each room based on the room area, see Table 2. The people and electricity load at each hour are calculated as the number of people \times occupant fraction, maximum electricity load \times electricity fraction respectively.

The zone ventilation function is used for single-zone ventilation. The zone mixing function calculates the air change and thermal change between zones. The natural ventilation airflow rate is calculated by the wind speed and thermal stack effect. The airflow by wind speed effect is calculated by Equation (3).

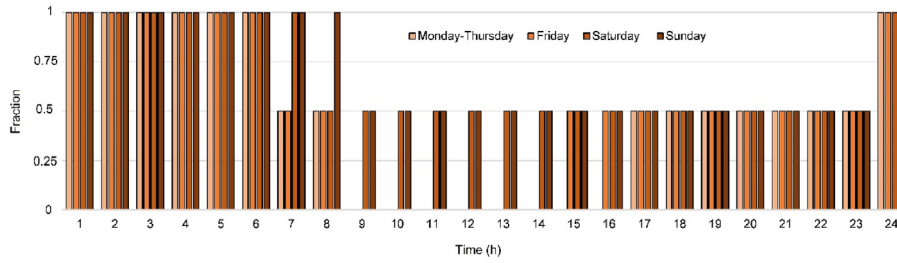


Fig. 4. The occupant fraction in functions of time.

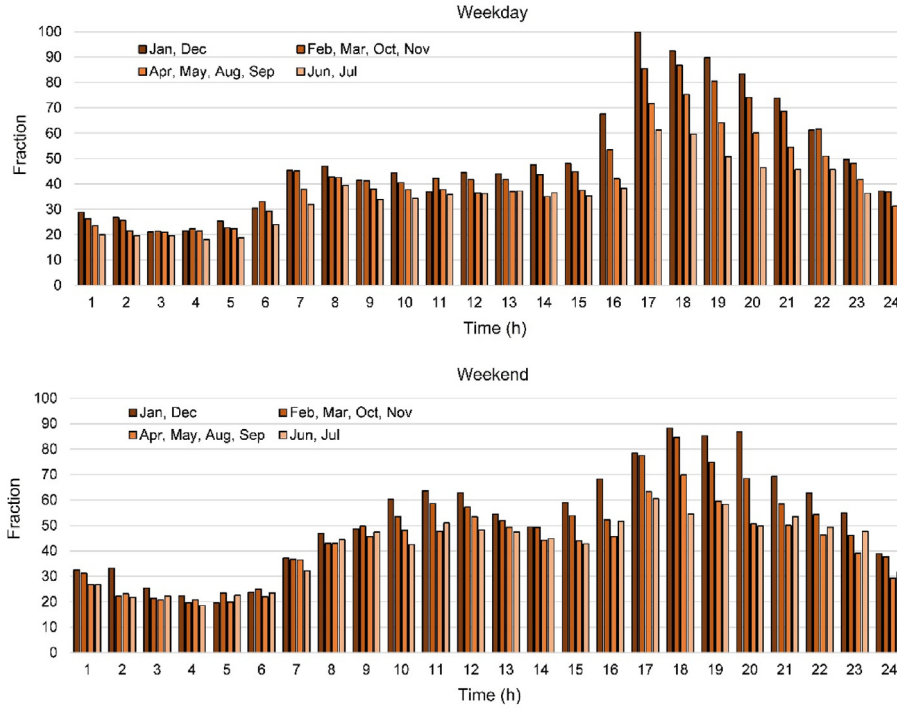


Fig. 5. The electricity fraction in functions of time.

Table 2

The distribution of internal heat gains.

	Room 1	Room 2	Room 3
Number of people	0.941	0.463	0.332
Maximum electricity load(W)	324.05	158.54	109.59

$$Q_w = C_w A f_{\text{schedule}} v \quad (3)$$

Where Q_w is the airflow rate driven by wind (m^3/s), C_w is the opening effectiveness, A is the opening area (m^2), f_{schedule} is the schedule of opening fraction, v is the local wind speed (m/s).

The opening effectiveness is calculated by the angle between the effective angle and real-time wind direction for each simulated time step, as shown in Equation (4).

$$C_w = 0.55 - \frac{|EffectiveAngle - WindDirection|}{180} \times 0.25 \quad (4)$$

The airflow rate driven by thermal stack effect Q_s is shown in Equation (5).

$$Q_s = C_s A f_{\text{schedule}} \sqrt{2g\Delta h(|T_i - T_o|/T_i)} \quad (5)$$

Where Δh is the height from midpoint of lower opening to the neutral pressure level (m); T_i is the zone air temperature ($^{\circ}\text{C}$); T_o is the outdoor air temperature ($^{\circ}\text{C}$); C_s is the discharge coefficient for opening, which is defined by Equation (6).

$$C_s = 0.4 + 0.0045|T_i - T_o| \quad (6)$$

The total airflow rate is calculated by Equation (7).

$$Q = \sqrt{Q_s^2 + Q_w^2} \quad (7)$$

2.1. Full-scale experimental test and model validation

The PCM WV is tested in the south surface of the façade lab at Aalborg University. The window is equipped with a ventilation system (including the ducts and valves) to create stable airflow in the window. The experiments include 3 parts: testing the pre-cooling ability of the PCM WV for night cooling application,

measuring the pre-heating ability of the PCMVW for solar energy storage application, and testing the reflection/absorption blinds and self-cooling mode of the VW. The PCM temperature, air temperature in the PCM heat exchanger and VW cavity are measured. The measurement points are shown in Fig. 6. Temperature sensors and pyranometers are set on the external surface to measure the outdoor air temperature and the solar radiation the façade receives. A weather station on the roof of the building is measuring the weather conditions, include the wind speed and wind direction.

The aim of the experiment is to validate the numerical model. The experiment thus simplified some of the control strategies. For the summer night cooling application, in the experiment the PCMVW is constantly ventilated. The same ventilation is set in the numerical model, as well as the same outdoor weather conditions and external shading for PCM. For the winter solar energy storage application, the ventilation and outdoor weather conditions are set for the experiment and numerical model of the PCMVW are set as the same as well. For the blinds control, only the VW part with the absorption/reflection blinds is ventilated and tested in the experiment. The corresponding blinds are added and the ventilation is only set in the VW in the numerical model.

2.2. Part 1: Night cooling application

The night cooling application experiment is done to measure the pre-cooling ability of the PCMVW during hot weather conditions. The PCM heat exchanger is shaded with external shading to avoid temperature rise by the sunlight. The ventilated window is not shaded during this experiment, see Fig. 7. The PCM is ventilated during the nighttime, to be cooled down by the cold outdoor air. It is then ventilated during the daytime, to pre-cool the ventilated high-temperature outdoor air. The test is done from 12th July–16th July 2017. Fig. 8 shows the measured outdoor weather conditions. The minimum outdoor air temperature for all the measured days

are below the PCM freezing temperature (20.7 °C), which is required for effective night cooling application.

Fig. 9 shows the PCM temperature, air temperature in the PCM cavity, air temperature in the VW cavity from both experiment and simulation results for night cooling application. It shows good agreements between the experiment and simulation results. The modeling average error for PCM temperature, PCM cavity, VW cavity is 5.0%, 5.7% and 5.4% respectively, which is calculated based on Equation (8). The modeling root mean square error (RMSE) for PCM temperature, PCM cavity, VW cavity is 1.0 °C, 1.3 °C and 1.5 °C respectively, which is calculated based on Equation (9). The weather input for the simulation is hourly data, which may cause a part of the discrepancy.

$$error = \left| \frac{\text{Experimental value} - \text{Simulation value}}{\text{Experimental value}} \right| \times 100\% \quad (8)$$

$$RMSE = \sqrt{\frac{\sum_{i=1}^N (\text{Experimental value}_i - \text{Simulation value}_i)^2}{N}} \quad (9)$$

2.3. Part 2: Solar energy storage application

The solar energy storage application aims at using the stored solar energy to pre-heat the low-temperature ventilation, typically during winter. The test is done from 02 to 07–2019 to 12-07-2019. In this test, the PCM stores the solar energy during the daytime (8:30–18:30), and releases the energy to pre-heat the ventilation during the night time (18:30–8:30), as illustrated in Fig. 10. The measured outdoor weather condition in Fig. 11 shows that the solar radiation levels of the measured days are all different. For some

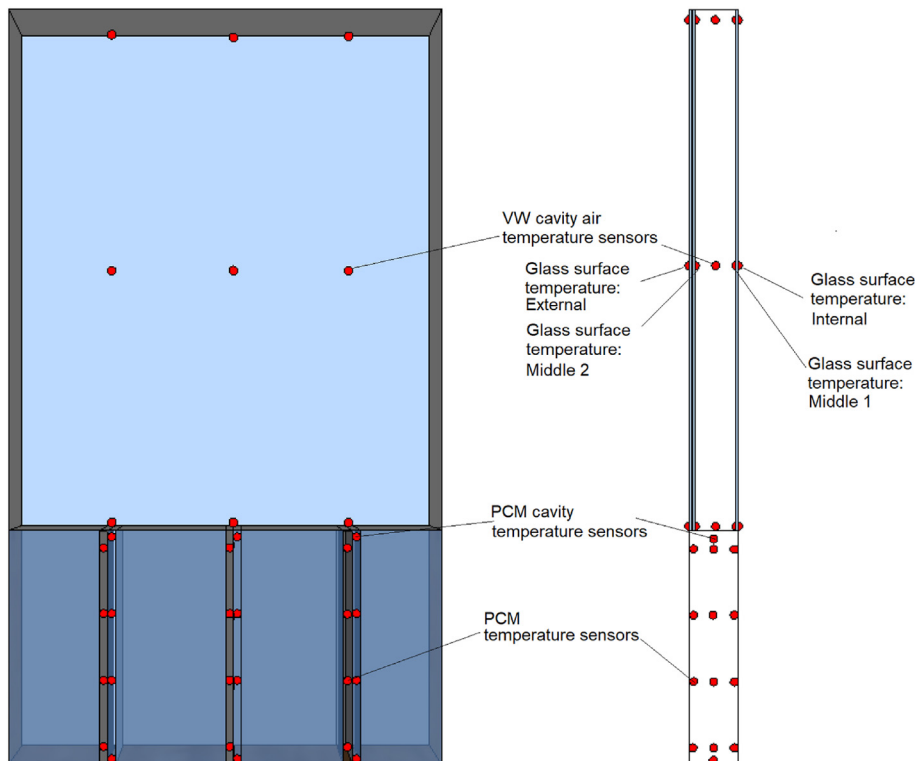


Fig. 6. The temperature sensors in the PCMVW.

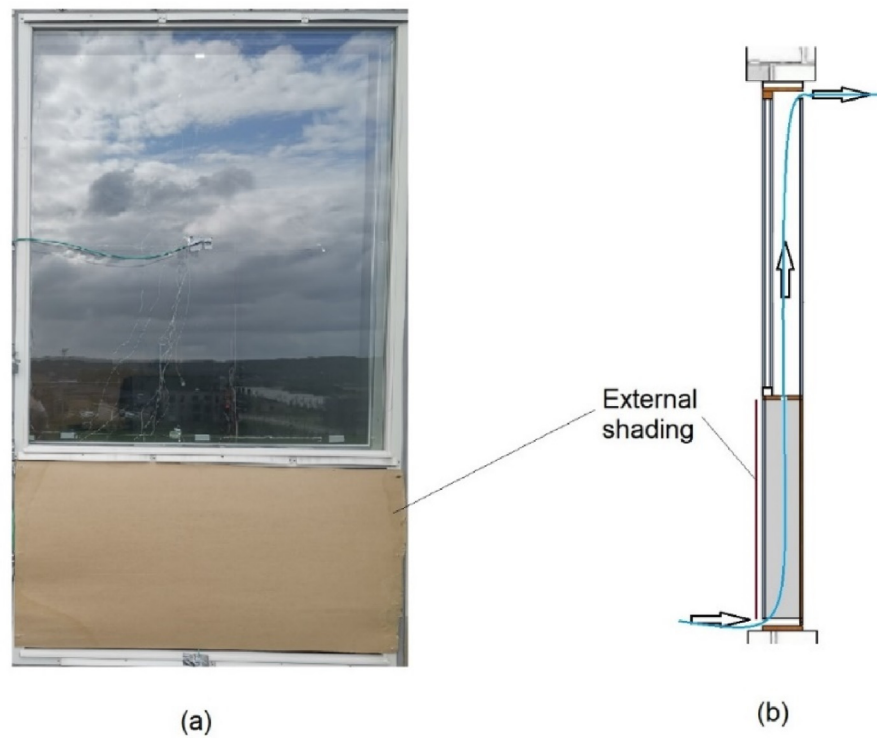


Fig. 7. The tested case for summer night cooling application. (a) Experimental setup; (b) sketch of the PCM window with external shading.

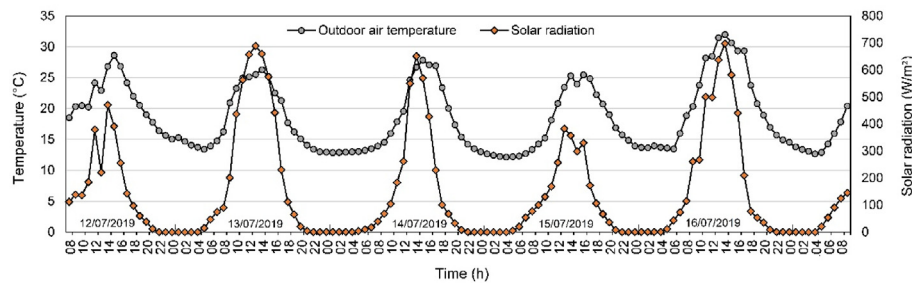


Fig. 8. Measured outdoor weather data for summer night cooling application.

days there is high solar radiation, for some other days the solar radiation is low.

Fig. 12 shows the PCM temperature, air temperature in the PCM cavity, air temperature in the VW cavity from both experiment and simulation results for solar energy storage application. Good agreements can be found between the experiment and simulation results. The modeling average error for PCM temperature, PCM cavity, VW cavity is 12.5%, 7.1% and 6.8% respectively. The RMSE for PCM temperature, PCM cavity, VW cavity is 2.4 °C, 1.7 °C and 1.7 °C respectively.

2.4. Part 3: Adding blinds for advanced VW control

A blind with two different functional sides is developed to improve the energy performance of the PCM window. One side of the blind is painted with a high reflection coating, while the other side is painted with a high absorption coating. Fig. 13 shows the occasions when the reflection/absorption side is applicable. For summer cooling application, using reflection shading can decrease the solar heat gain from the VW to the room, as well as decrease the inlet air

temperature for room ventilation. For the winter solar energy storage application, using absorption blind can add heat to the VW, thus increases the ventilation preheating effect. For the cases when the indoor air temperature is too high, using shading in cooperation with self-cooling natural ventilation can effectively decrease the temperature of the VW, thus decreases the heat gain through the window. The blinds not only regulates the air temperature in the VW, but also act as an effective way of the daylight control of the room, to avoid the direct sunlight exposure of the occupants from a low hanging winter sun.

In this experiment, only the VW with reflection/absorption blinds are tested and compared with the numerical model. The PCM is not ventilated or tested.

The experiment tests the VW with reflection/absorption blind under natural/mechanical ventilation respectively. The VW with reflection blind under natural ventilation is tested in 14–10–2019. The experiment is not done in continuous days because there are no continuous sunny days during the tested period. Fig. 14 shows the outdoor wind speed and wind direction. Fig. 15 shows the outdoor air temperature, solar radiation on the vertical surface and

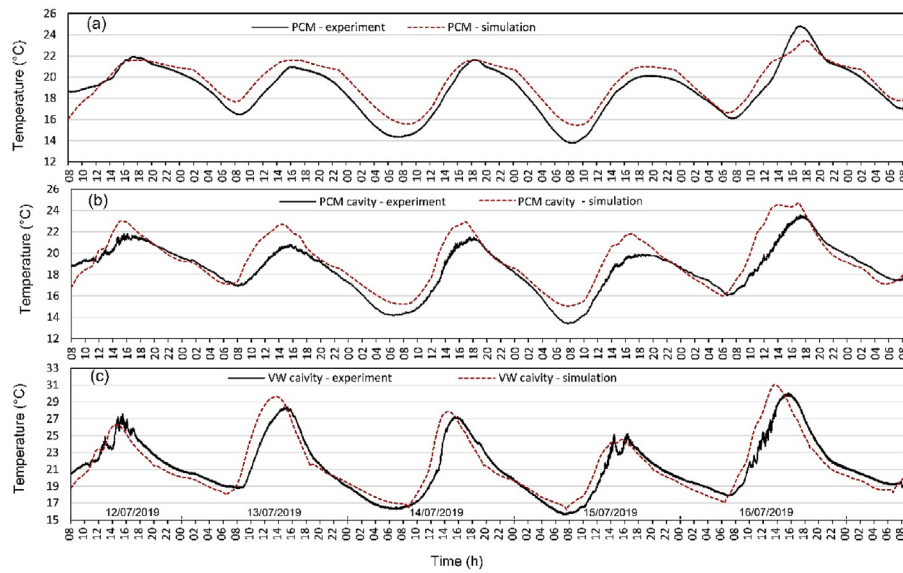


Fig. 9. Model validation of summer night cooling application. (a) PCM temperature; (b) air temperature in the PCM cavity; (c) air temperature in the VW cavity.

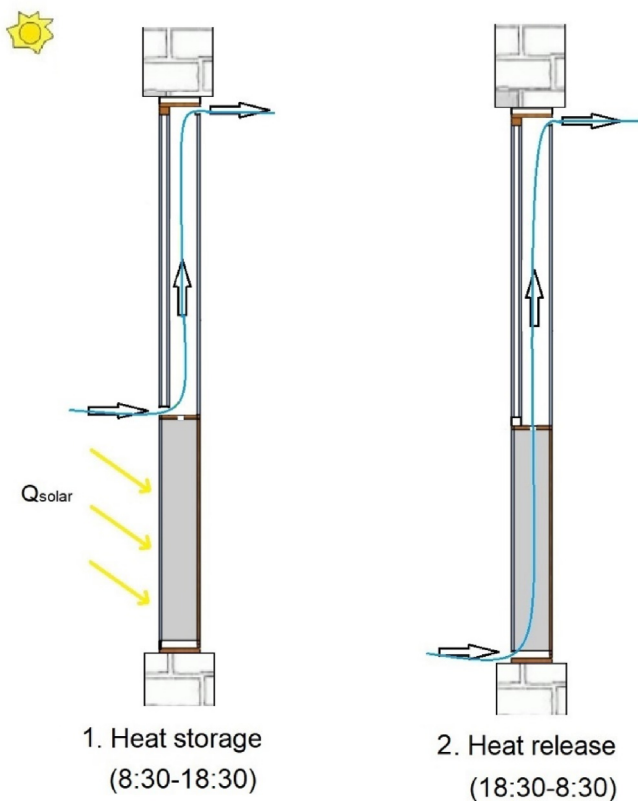


Fig. 10. The tested cases for winter solar energy storage application.

temperature of the different glass surfaces. The positions of the temperature sensors are in Fig. 2. There are good agreements between the measured glass surface temperature and simulated results. The modeling error for internal, middle 1, middle 2, external sensors is 9.8%, 9.4%, 13.1% and 8.2% respectively. The RMSE for internal, middle 1, middle 2, external sensors is 2.1 °C, 2.0 °C, 2.7 °C and 1.4 °C respectively.

The VW with absorption blind under natural ventilation is

tested on 31-10-2019. Fig. 16 shows the outdoor wind condition. Fig. 17 shows the outdoor air temperature, solar radiation on the vertical surface and temperature of the different glass surfaces. The same trends can be found with the experimental data and simulation results. The modeling error for internal, middle 1, middle 2, external sensors is 8.1%, 9.9%, 8.8% and 11.2% respectively. The RMSE for internal, middle 1, middle 2, external sensors is 2.1 °C, 2.9 °C, 2.8 °C and 1.6 °C respectively.

Comparing the 3 experiments, it is seen that the model for night cooling application has the best fit with the experimental results. One possible reason is that the model is less influenced by solar radiation, while the other 2 models are more influenced by solar radiation, especially for blinds testing. The errors come from the measurement uncertainty, uncertainties of material properties provided by the manufacturer, and the unavoidable personal error (for example, the blind is not possible to close at 100% close position to avoid sunlight go through the gaps). Moreover, the hourly average values of outdoor weather conditions are used in the model, which can be a big contribution to the model uncertainty.

3. PCM ventilation performance

The PCM/VW and its numerical model are developed and tested. However, the cooling/heating ability of the PCM/VW comparing to other ventilation systems remains to be examined. In this chapter, the building with PCM/VW is compared with the same building with other 2 ventilation systems: ventilated window without PCM (VW, no PCM) and normal window without both ventilated window and PCM (no VW, no PCM). The heating and cooling energy demands of the building are compared for summer night cooling and winter solar energy storage applications respectively.

3.1. Summer night cooling effectiveness

The night cooling application is active during May–October. 3 ventilation systems and their ventilation cooling abilities are compared. The windows in the 3 systems have the same configuration and material constitutes. Fig. 18 shows the system composition and operation strategies of the 3 systems. The PCM/VW (Fig. 18(a)) has 3 operation modes: the heat removal mode during the night time, where the cold outdoor air ventilate through the

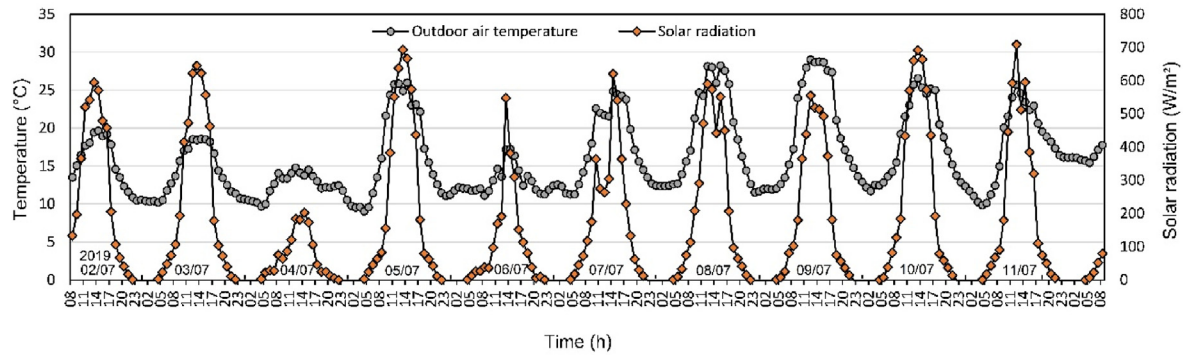


Fig. 11. Measured outdoor weather data for winter solar energy usage application.

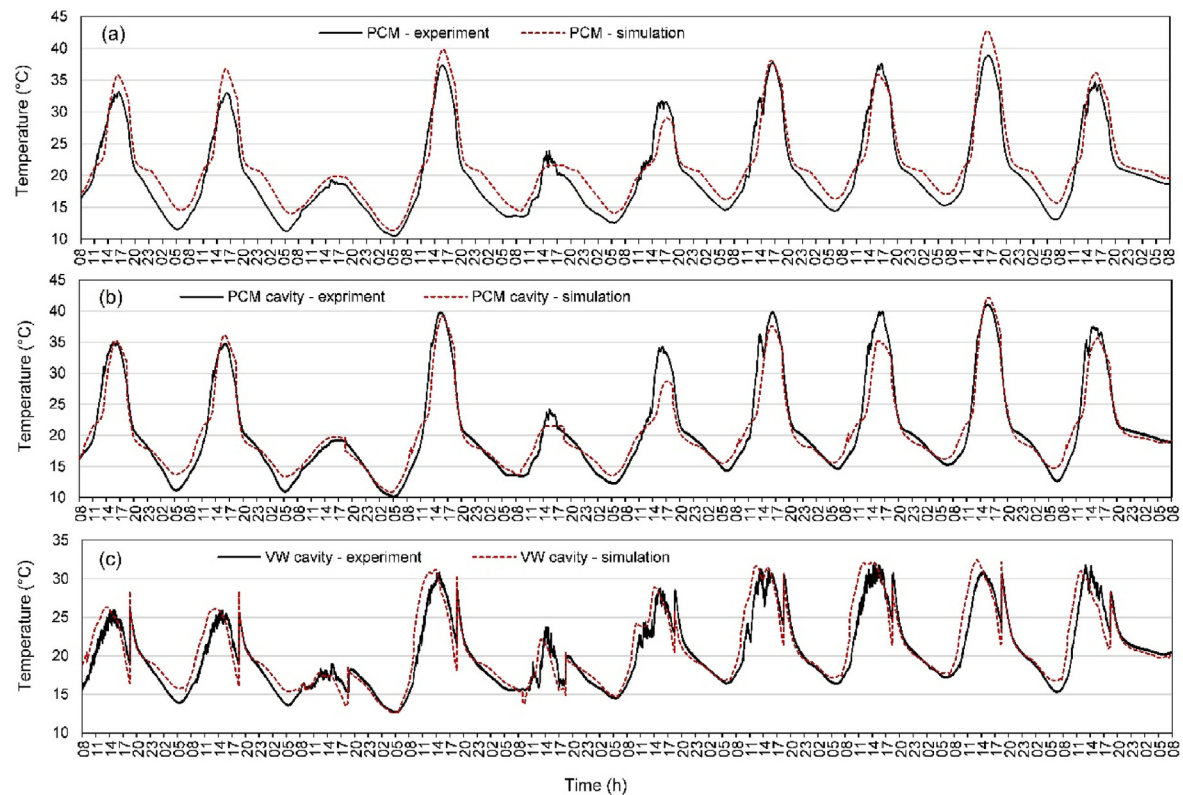


Fig. 12. Model validation of winter solar energy usage application. (a) PCM temperature; (b) air temperature in the PCM cavity; (c) air temperature in the VW cavity.

PCM to cool it down; the ventilation pre-cooling mode, where the PCM cools down the ventilation where the indoor air temperature is too high; the heat mode, where the ventilation only goes through the double window (which is heated up by solar radiation) when the indoor air is overcooled and heating is needed. As references, the VW, no PCM (Fig. 18(b)) and no VW, no PCM (Fig. 18(c)) systems are ventilated with the same time schedule and airflow rate.

Fig. 19 shows the room ventilation inlet air temperature from 1st August– 7th August. For room 1 (southwest room), the no VW, no PCM system has the lowest inlet air temperature (which is close to the outdoor air temperature), and the VW, no PCM system has the highest inlet air temperature. For room 2 (northeast room), the inlet air temperatures of the 3 systems show the same trends, and are much lower than room 1 with the same ventilation system (except for no VW, no PCM system, which has the same inlet air temperature for the 2 rooms). It is because the windows facing

southwest have more heat gains than the windows facing northeast.

Fig. 20 shows the inner glass surface temperature of the 3 systems from 1st August– 7th August. The higher the inner glass surface temperature, the higher the amount of heat gain the room gets from the window. For both rooms, the no VW, no PCM system has the highest glass surface temperature, and the PCMVW system has the lowest inner glass surface temperature. The no VW, no PCM system has no ventilation in the window cavity, thus the heat is gathered in the air inside the cavity, which increases the glass surface temperature. While for the PCMVW, the PCM cools down the ventilation, and the relatively low-temperature air potentially cools down the glass surface temperature.

The ventilation inlet air temperature and the inner glass surface temperature are not showing the same trend. This indicates that none of them can be used as an indicator to compare the ventilation

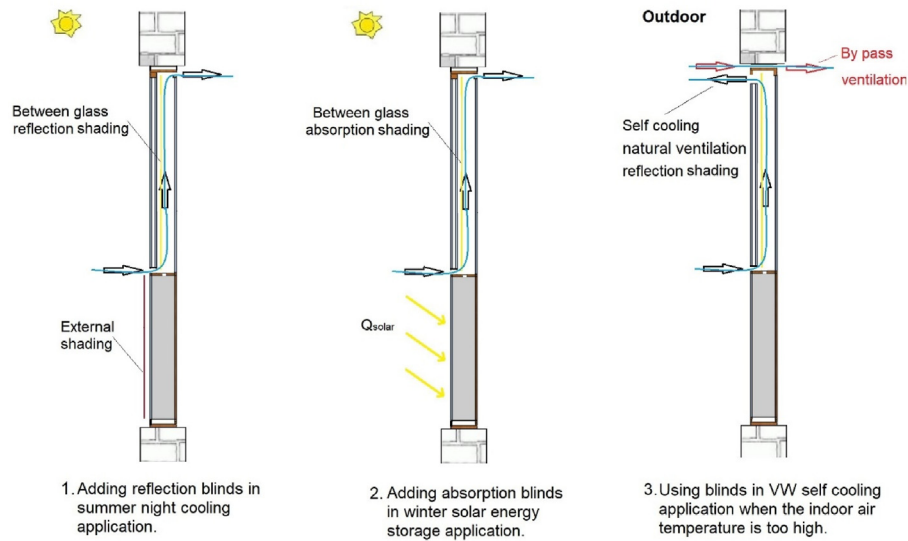


Fig. 13. The advanced strategy control with blinds.

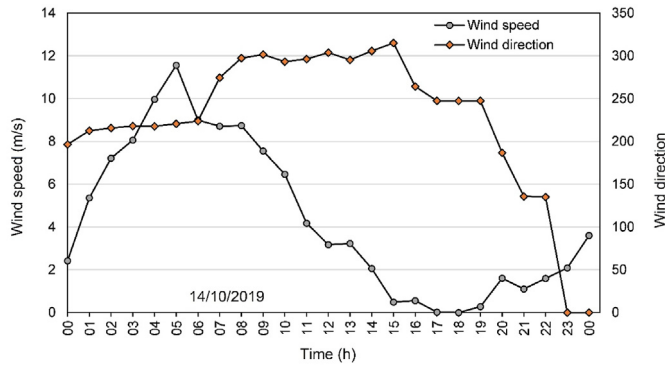


Fig. 14. The outdoor wind condition of the tested day for natural ventilation with reflection blind.

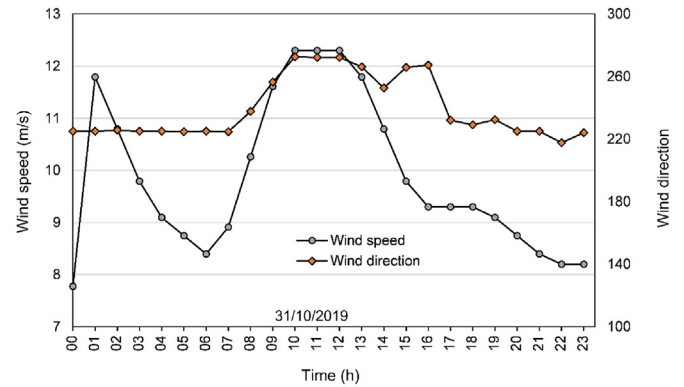


Fig. 16. The outdoor wind condition of the tested day for natural ventilation with absorption blind.

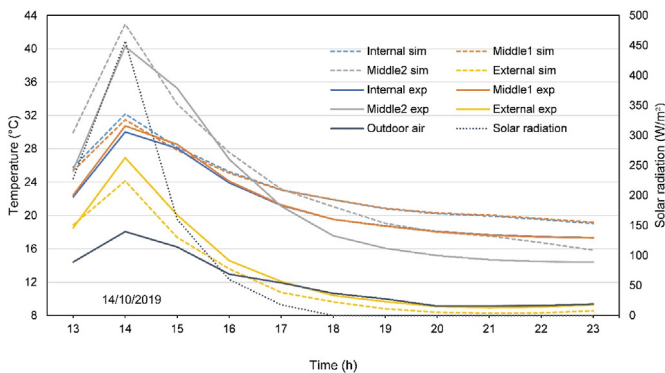


Fig. 15. The model validation of double window natural ventilation: with reflection blind for the between-glass blind.

performance. The energy demands of the building with the 3 systems for the whole summer period are calculated and shown in Fig. 21. For both rooms, the VW, no PCM system provides the highest cooling energy demand for all the simulated months, which indicates a poor cooling ability of the VW. The PCMVW provides the lowest cooling energy demand. The heating energy demand is quite

low and is present in October. For room 1, the PCMVW reduction in cooling energy demand is 46% compared to VW, no PCM system, and the reduction is 27% compared to the no VW, no PCM system. For room 2, the PCMVW reduction in cooling energy demand is 51% and 38% compared to the other two systems respectively. Room 3 has the same orientation of the external wall as room 2, and the sizes of the two rooms are similar. As a result, the energy demand per square meter floor area is similar, therefore it is not discussed here.

3.2. Winter solar energy storage effectiveness

The solar energy storage application is active from November–April. The similar 3 systems and their ventilation heating abilities are compared. Fig. 22 shows the system compositions and operation strategies of the 3 systems. The PCMVW (Fig. 22(a)) has 2 operation modes: the heat release mode, where the ventilation pre-heating is operated when the room is in low temperature; the overheating preventing mode, where the bypass and self-cooling ventilation is operated when the indoor air temperature is too high; meanwhile, the PCM stores the solar energy when the sunlight is available. The VW, no PCM system (Fig. 22(b)) has the same ventilation schedule as the PCMVW except there is no PCM heat

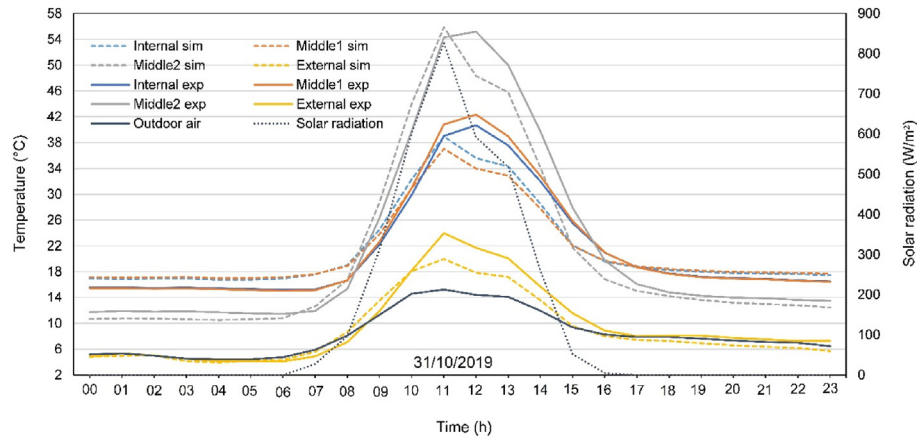


Fig. 17. The model validation of double window natural ventilation: with absorption blind for the between-glass blind.

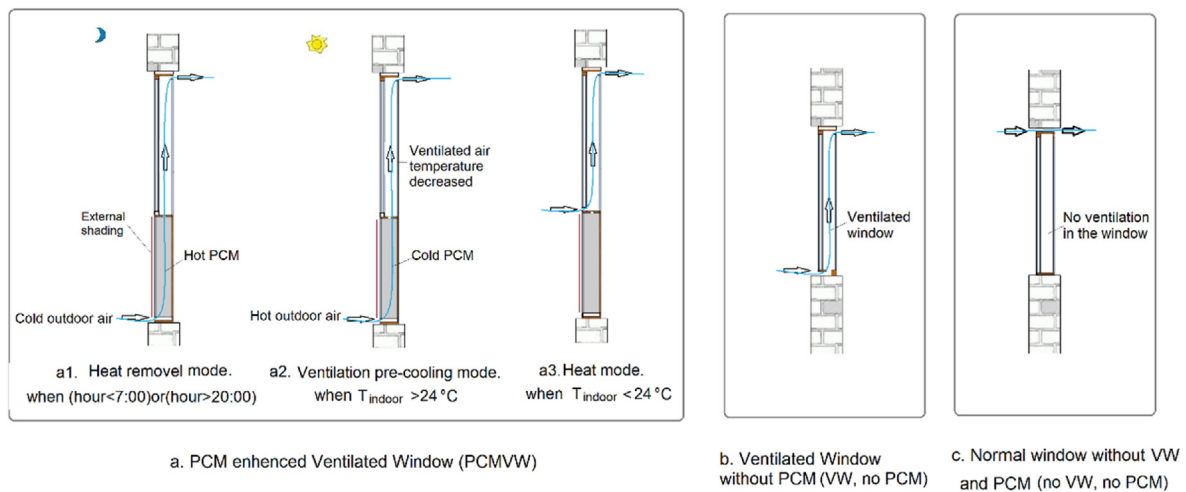


Fig. 18. Compare of PCMVW with 2 other ventilation systems for summer night cooling application.

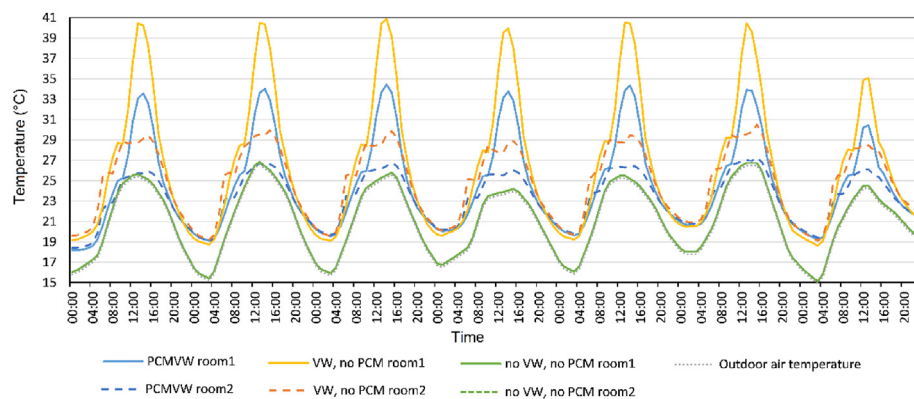


Fig. 19. The room ventilation inlet air temperature of the 3 ventilation systems from 1st August– 7th August for summer night cooling application.

exchanger. The no VW, no PCM system (Fig. 22(c)) is only ventilated with bypass ventilation.

Fig. 23 shows the room ventilation inlet air temperature during the period 5th February– 23rd February. For both rooms, the PCMVW has the highest inlet air temperature. The no VW, no PCM system has the lowest inlet air temperature. With the same ventilation system, the inlet air temperature of room 1 is much

higher than room 2 (except for no VW, no PCM system, which has the same inlet air temperature for the 2 rooms). The windows in southwest façade have more solar heat gains than in northeast façade.

Fig. 24 shows the inner glass surface temperature of the 3 ventilation systems during the period 5th February– 13th February. For room 1 (southwest room), the no VW, no PCM system has the

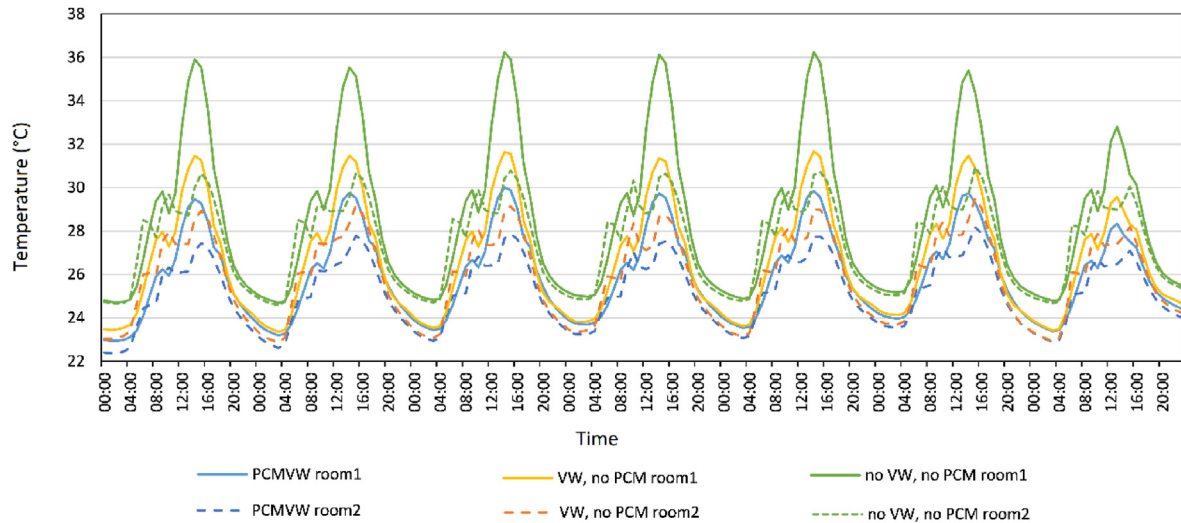


Fig. 20. The inner glass surface temperature of the 3 ventilation systems from 1st August–7th August for summer night cooling application.

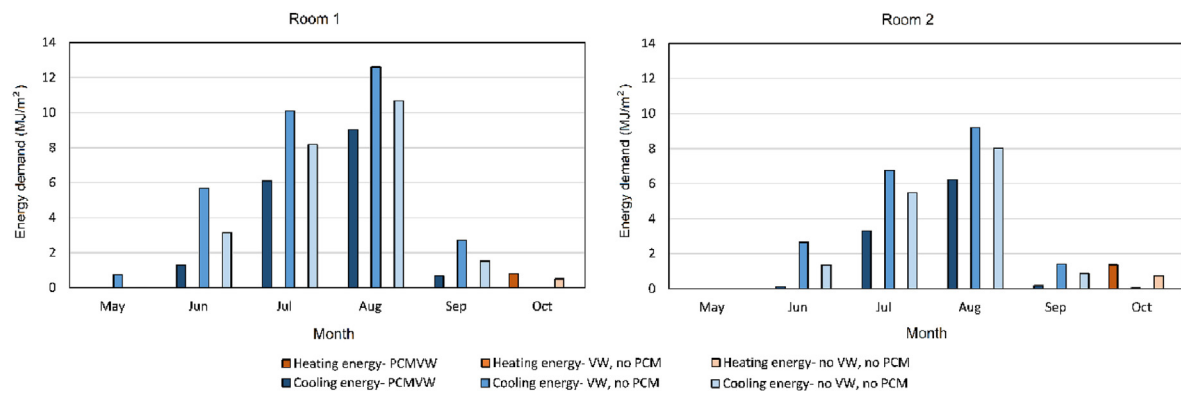


Fig. 21. The building energy demand with the 3 different ventilation systems for summer night cooling application.

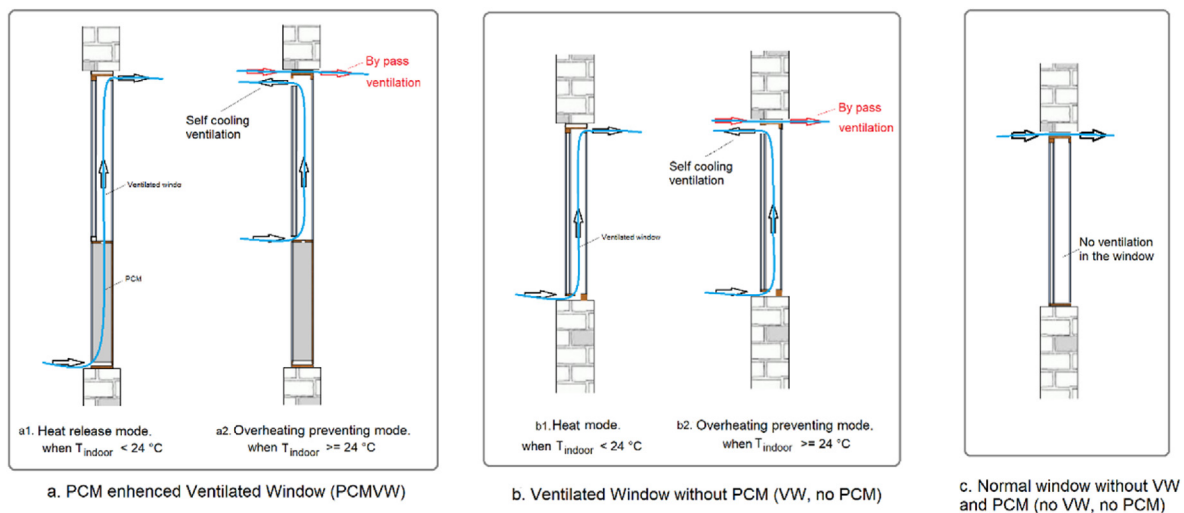


Fig. 22. Compare of PCMVW with 2 other ventilation systems for winter solar energy storage application.

highest inner glass surface temperature, and the VW, no PCM system has the lowest inner glass surface temperature. However, for room 2 (northeast room), the no VW, no PCM system has the

highest inner glass surface temperature, while the PCMVW and the no VW, no PCM systems have a similar inner glass surface temperature for most of the time.

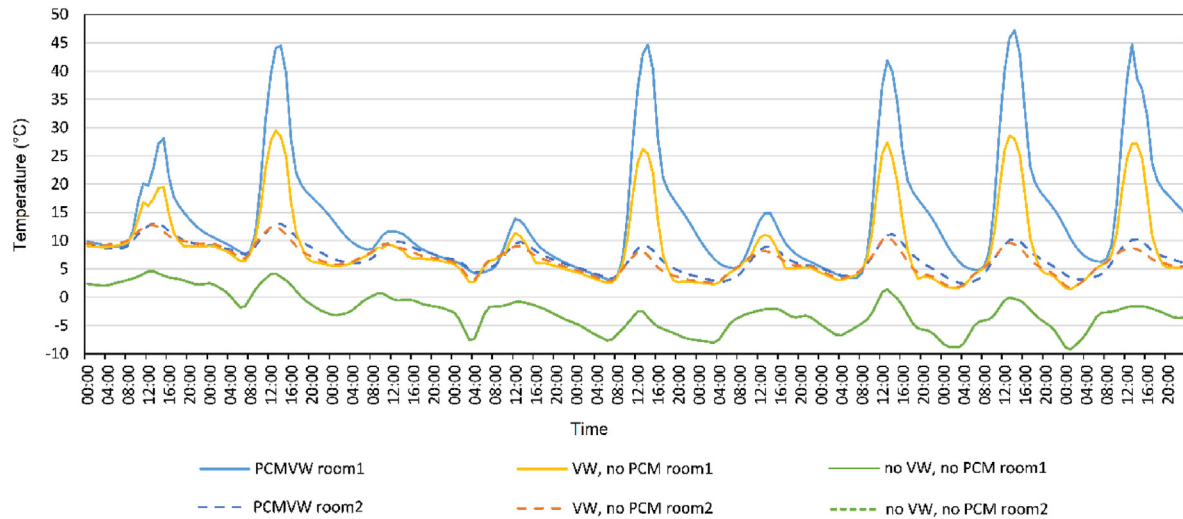


Fig. 23. The room ventilation inlet air temperature of the 3 ventilation systems from 5th February– 23rd February for winter solar energy storage application.

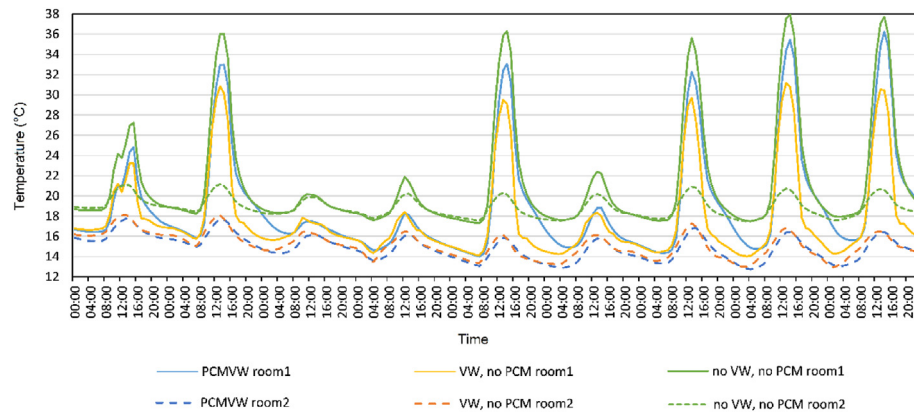


Fig. 24. The inner glass surface temperature of the 3 ventilation systems from 5th February– 23rd February for winter solar energy storage application.

For room 2 (northeast room), when comparing the PCM VW system with the VW, no PCM system, both the ventilation inlet air temperature and the inner glass surface temperature are similar. The PCM does not have a high ventilation heating potential for windows in northeast façade for some winter days, due to the low solar radiation received. However, the situation will be changed during March and May, when the received solar radiation level on the northeast façade increases. This is shown in the energy demand comparison, which can be seen in Fig. 25.

The energy demands of the building with 3 different systems are calculated separately, as shown in Fig. 25. For both rooms, the PCM VW provides the lowest energy demand, and the no VW, no PCM system the highest energy demand. For room 2, the energy demand of the PCM VW and the VW, no PCM systems are similar in December and January. Compared to the no VW, no PCM system and the VW, no PCM system, for room 1, the PCM VW system reduces the heating energy demand by 29% and 48% respectively; for room 2, the PCM VW system reduces the heating energy demand by 10% and 28% respectively.

4. Control strategy development

The primitive control strategies of the PCM VW shown in Figs. 7 and 10 can risk the room with overheating, due to the direct solar

heat gain through the window, or the excessive heat gain from the ventilation. The control strategy shown in Fig. 18(a) has too high room ventilation inlet air temperature during summer, which can be improved by adding shading control. This section develops control strategies to improve the pre-cooling efficiency of the PCM VW. The thermal and energy performance of the PCM VW with different control strategies are analyzed by the numerical model proposed in Section 2.

4.1. Summer night cooling control strategies

Three control strategies are developed for summer night cooling application. Strategy 1 increases between glass reflection shading for the VW, to avoid high solar heat gain from the VW to the room, as seen in Fig. 26. The heat mode is added as a part of the control strategy, in case the room is overcooled and room heating is needed. Based on strategy 1, strategy 2 improves the cold release mode by ventilating directly from the PCM heat exchanger to the room. The VW is self-cooled with natural ventilation, to further avoid its temperature rise by solar radiation, as shown in Fig. 27. Based on strategy 2, strategy 3 differentiates the heating/cooling setpoint, and adds a bypass mode when the indoor air temperature is in the comfortable range, see Fig. 28.

Fig. 29 shows temperature of the primitive strategy > strategy

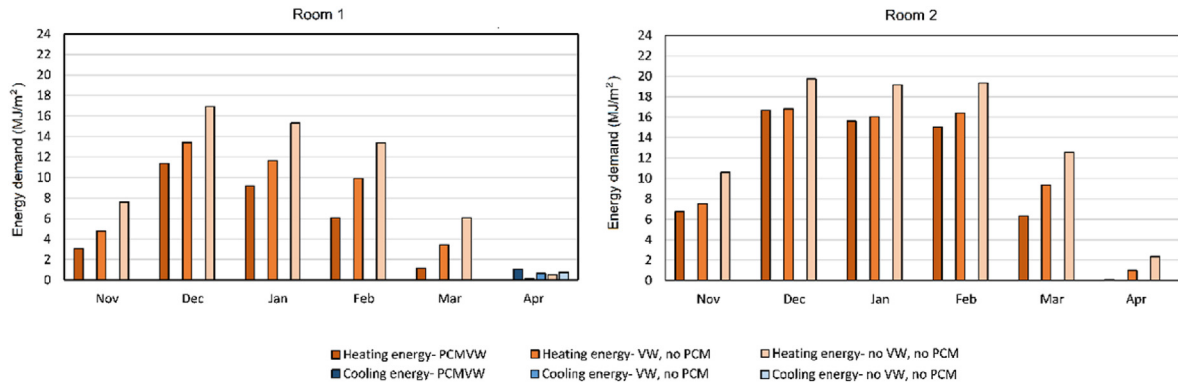


Fig. 25. The building energy demand with the 3 different ventilation systems for winter energy storage application.

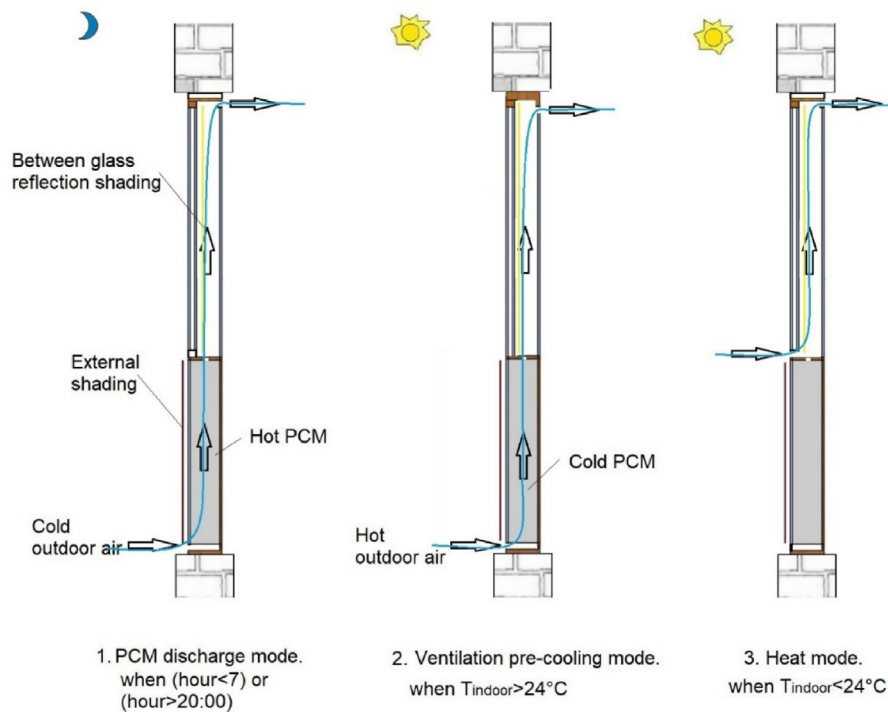


Fig. 26. The summer night cooling application control strategy 1.

2 > strategy 1 > strategy 3. The PCM temperature of strategy 3 is the lowest, for the reason that during the daytime, the ventilation time through PCM is the shortest compared to other control strategies. For 5th August – 7th August, the PCM temperature of the 4 strategies are similar. The probable reason is that the night time outdoor air temperature is too high to cool the PCM the PCM temperature of the PCM/VW under different control strategies. For both rooms, the PCM down below 21°C .

The ventilation inlet air temperature of the 4 control strategies are quite different (as shown in Fig. 30), even though for some days the PCM temperature are similar. For both rooms, the inlet air temperature of primitive strategy > strategy 1 > strategy 3 > strategy 2. For both the primitive strategy and strategy 1, the inlet air temperature of room 1 is much higher than room 2, due to the higher heat gain in the cavity of the ventilated window in room 1. For strategy 2, the ventilation inlet air temperature of the 2 rooms are similar, except 2nd August. Similarly, for strategy 3, the ventilation inlet air temperature of the 2 rooms are similar, except 3rd

August, when the PCM temperature of the 2 rooms show a bigger difference.

In comparison, strategy 3 has the lowest PCM temperature for both rooms. However, strategy 2 has the lowest ventilation inlet air temperature. The possible reason is that strategy 2 utilized the cooling ability of the PCM more than strategy 3. Consequently, strategy 2 has the least room energy demand, as seen in Fig. 31.

Fig. 31 shows the monthly energy demand using the 3 different control strategies for summer night cooling application. In general, room 1 has a higher energy demand than room 2, due to its orientation (southwest). Control strategies 1, 2 and 3 have less energy demand than the primitive strategy for all the simulated months. Control strategy 3 has slightly higher energy demand than strategy 2, due to the extra energy needed to handle the outdoor air temperature to the thermal comfort temperature during bypass mode. However, the difference between the two control strategies is quite small. The application is robust for temperature setpoint. From the overall energy demand of the system, the conclusion can

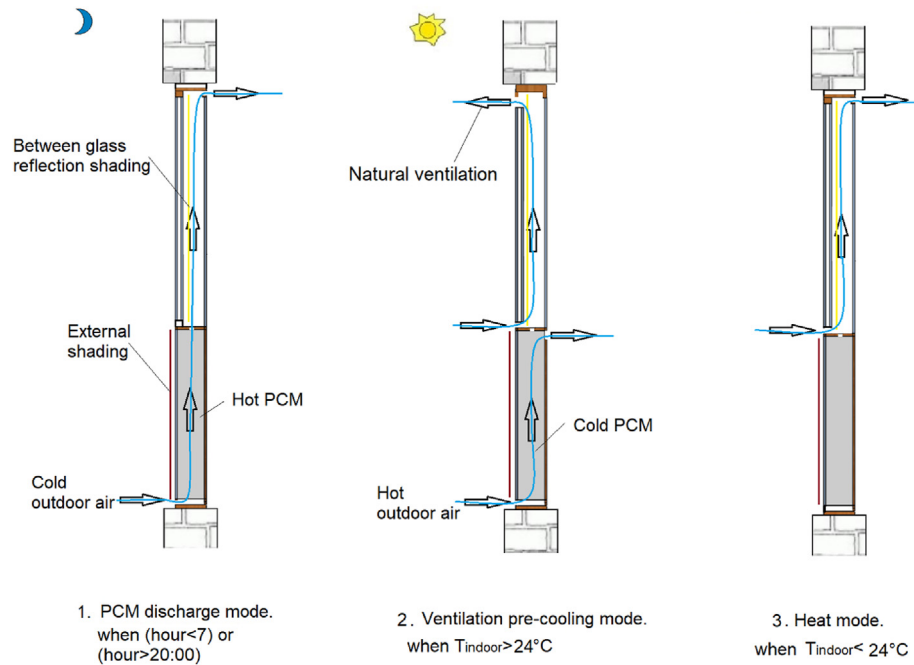


Fig. 27. The summer night cooling application control strategy 2.

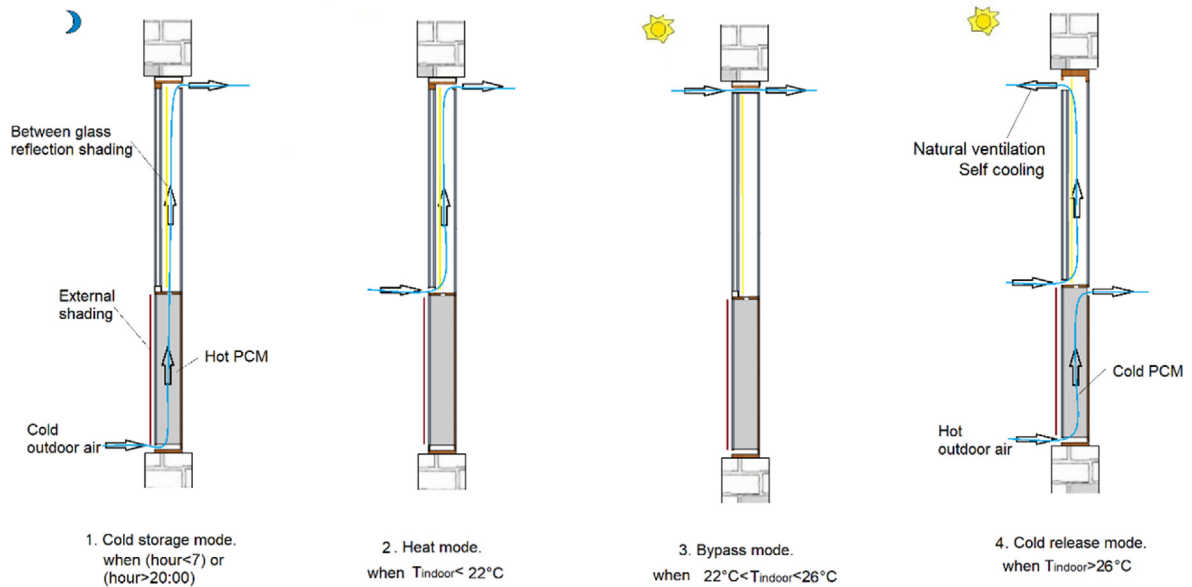


Fig. 28. The summer night cooling application control strategy 3.

be drawn that the optimized control strategy is strategy 2. Compared to the primitive strategy, the developed control strategy (strategy 2) saves 62.3% of the energy for the room with windows facing southwest, and 58.2% of the energy for the room with windows facing northeast.

4.2. Winter solar energy usage strategies

For further improvement, 3 more control strategies are developed for the winter control strategy. Strategy 1 (in Fig. 32) adds between glass absorption shading to increase the heat gain from the VW. The VW ventilation is operating in heat storage mode, to

make use of the hot air in the VW for room ventilation. Moreover, to avoid room overheating, the overheating preventing mode is added by introducing double window self-cooling and bypass ventilation. Based on strategy 1, strategy 2 (in Fig. 33) changes the heat release mode by ventilating directly from the PCM heat exchanger to the indoor room. Similarly, strategy 3 has a different heating/cooling setpoint, and adds a bypass mode when the indoor air temperature is in the comfortable range, see Fig. 34.

The PCM temperature in the PCMVW under different control strategies from 5th February–13th February are similar for each of the 2 rooms, except for some days the primitive strategy has the highest PCM temperature, which is shown in Fig. 35. In addition,

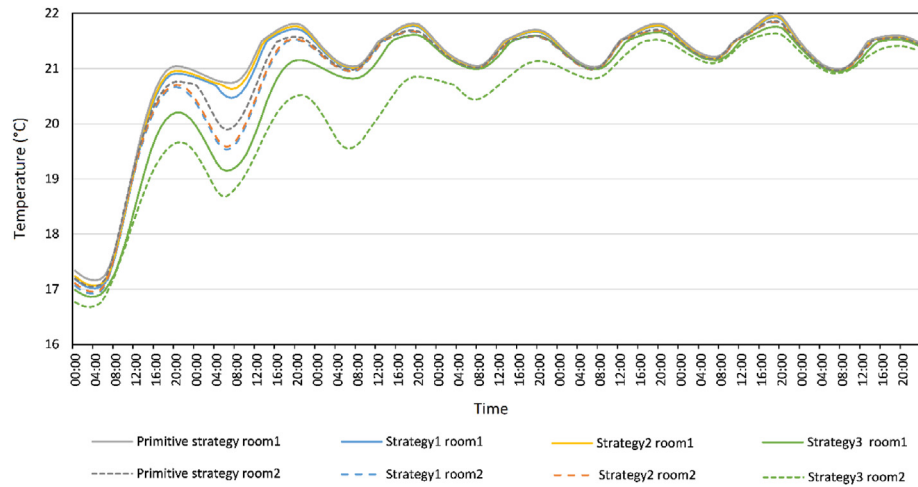


Fig. 29. The PCM temperature in the PCMVW using different control strategies from 1st August– 7th August.

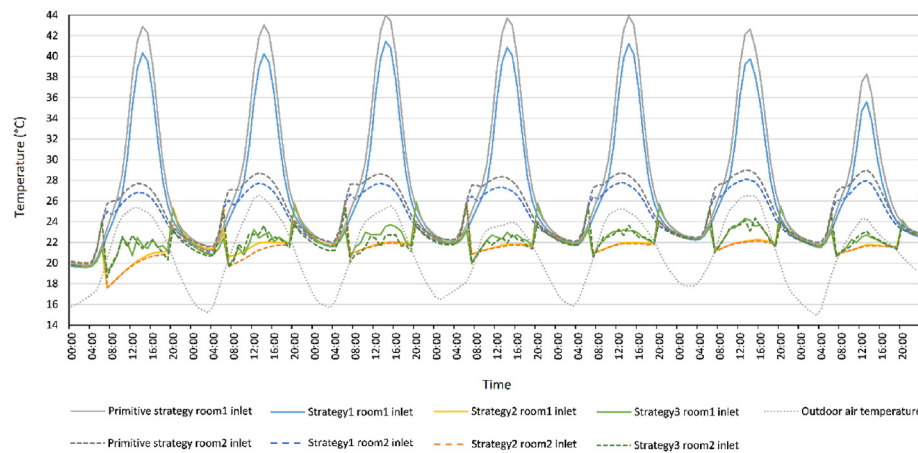


Fig. 30. The ventilation inlet air temperature of the PCMVW using different control strategies from 1st August– 7th August.

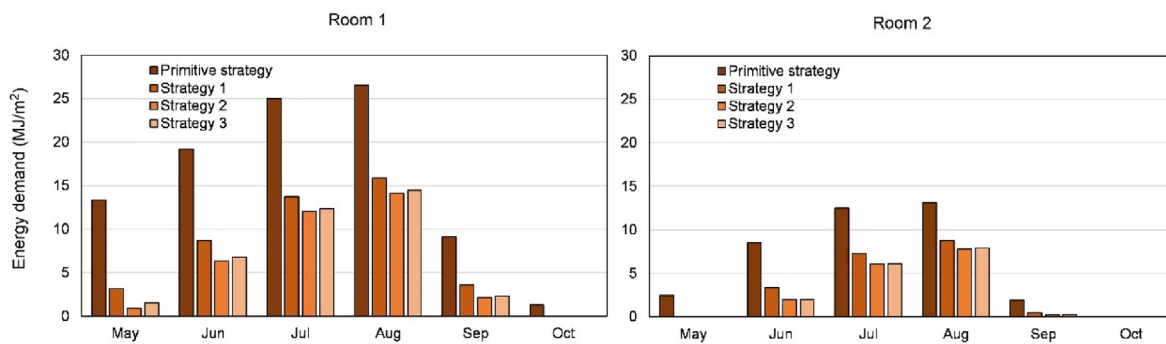


Fig. 31. The energy demand using different control strategies for summer night cooling application.

room 1 has a much higher PCM temperature than room 2. It indicates that the PCM temperature is more related to solar radiation and is robust against the control strategies.

The ventilation inlet air temperature, on the contrary, has some differences among the 4 control strategies, as shown in Fig. 36. For room 1, the primitive strategy has the highest inlet air temperature, strategy 1 and 3 have similar inlet air temperature, except during the afternoon, strategy 3 has a lower inlet air temperature, due to

the bypass mode. Strategy 2 has the lowest inlet air temperature in most of the days, especially for the days when the PCM temperature is low. It is due to the heat in the double window is not added to the ventilation during the heat release mode. For room 2, the ventilation inlet air temperature of primitive strategy > strategy 1 = strategy 3 > strategy 2 for most of the time.

Fig. 37 shows the monthly energy demand of models using different control strategies for winter solar energy storage

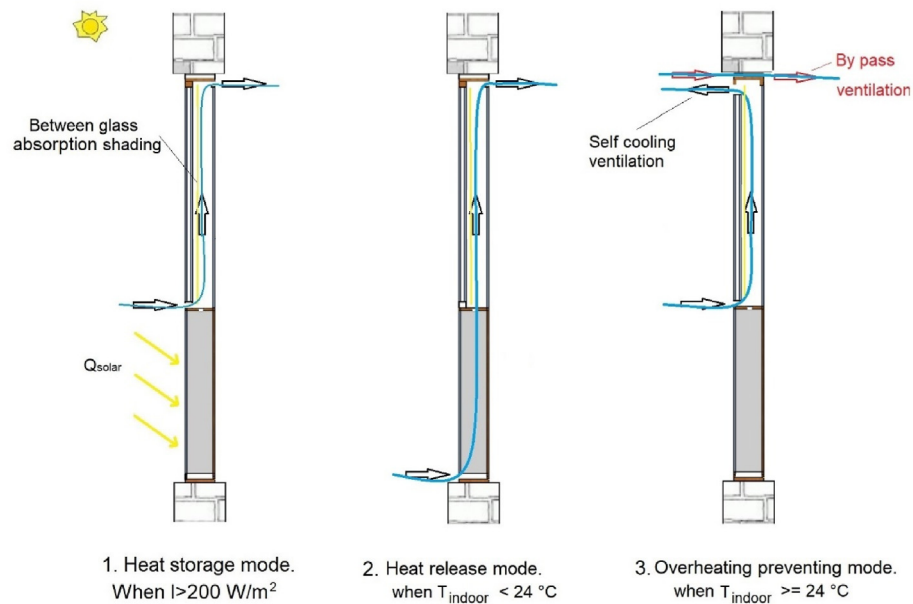


Fig. 32. The winter solar energy storage application control strategy 1.

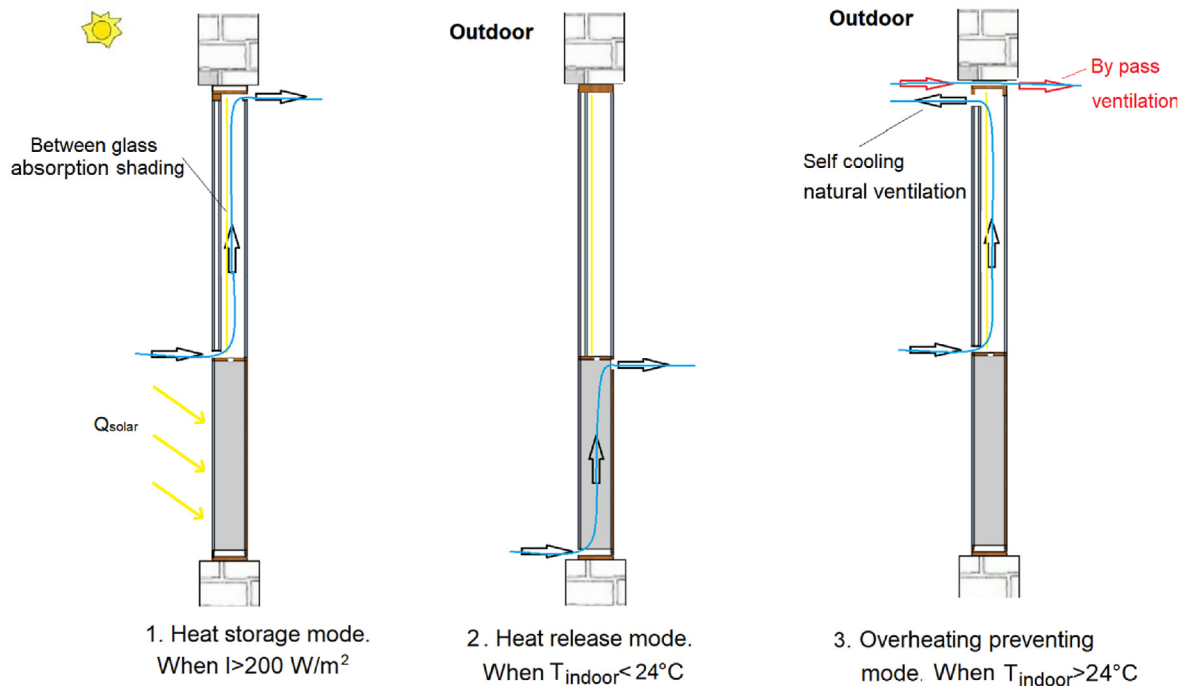


Fig. 33. The winter solar energy storage application control strategy 2.

application. It shows that compared to the primitive strategy, strategy 1 has the least energy demand for all the simulated months. The primitive control strategy has the highest inlet air temperature. However, it is lacking in the overheating preventing mode, which potentially increased the cooling energy demand. Strategy 2 has the highest energy demand for all the simulated months. The reason is that for both rooms, strategy 2 has the lowest ventilation inlet air temperature, due to the heat in the window cavity is not added into the ventilation. Compared to the primitive strategy, the developed control strategy (strategy 1) saves 9.4% of

the energy for the room with windows facing southwest, and 4.4% of the energy for the room with windows facing northeast.

The control strategy development of summer night cooling application has more improvement in energy efficiency than winter solar energy storage application. The potential reason may be that the amount of heat from the solar radiation is limited during winter, so that the PCM is not heated up at very high temperatures in most of the days. However, the air from the PCM heat exchanger is still much higher than the outdoor air temperature. Overall, the winter application is more robust regardless of what control

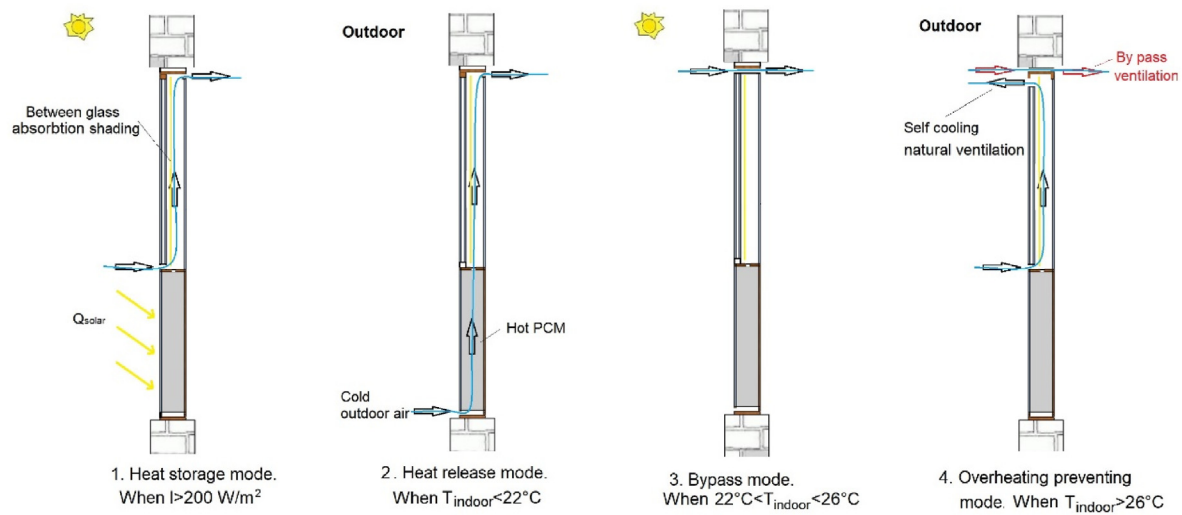


Fig. 34. The winter solar energy storage application control strategy 3.

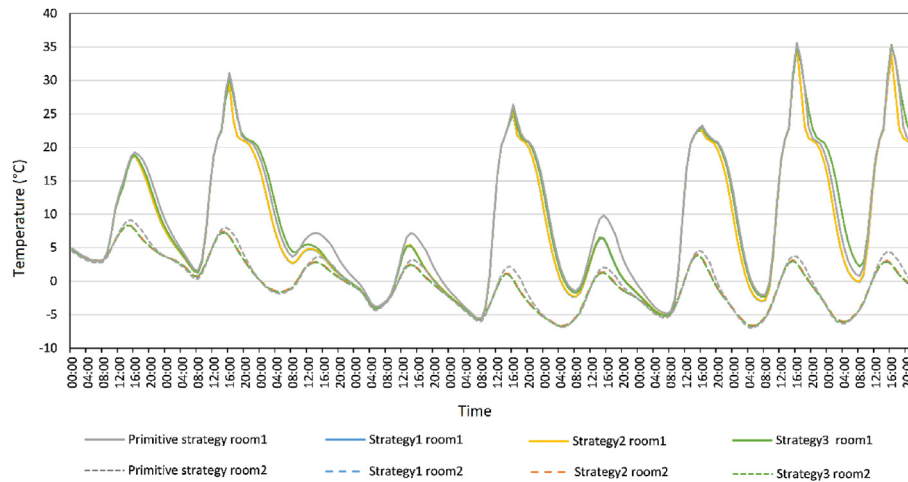


Fig. 35. The PCM temperature in the PCMVW using different control strategies from 5th February- 13th February.

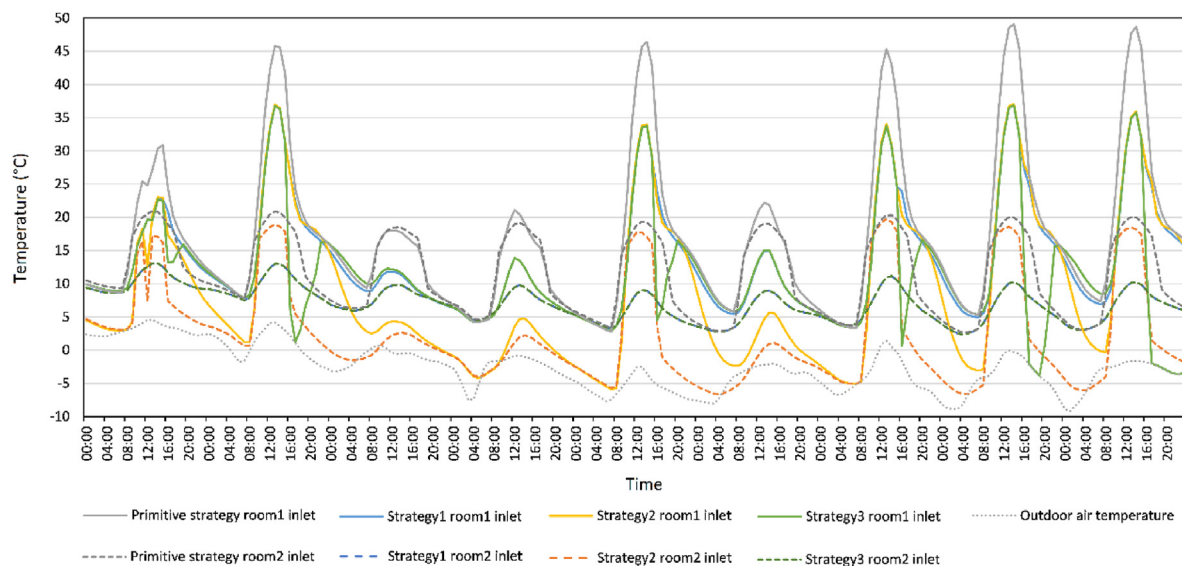


Fig. 36. The ventilation inlet air temperature of the PCMVW using different control strategies during 5th February- 13th February.

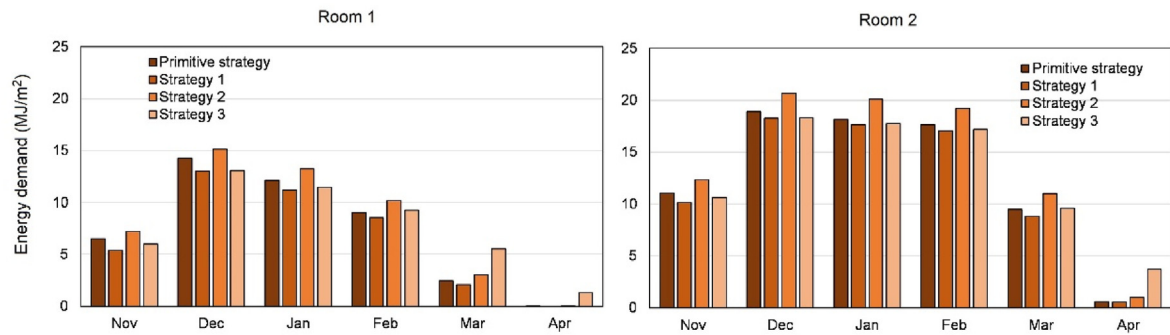


Fig. 37. The energy demand using different control strategies for winter solar energy storage application.

strategy is used.

5. Conclusions

This paper proposed a PCM enhanced ventilated window (PCM/VW) system for ventilation pre-treatment purposes. The system works in both summer and winter with different control strategies. In the summer night cooling application, the PCM decreases its temperature by night ventilation, and later it is used for ventilation pre-cooling purpose, by cooling down the high temperature ventilated air during the daytime. In winter solar energy storage application, the PCM stores solar energy during a sunny day, and it is later used for ventilation preheating, by heating up the low temperature ventilated air (mostly during the night time). This paper aims to study the working principle of the PCM/VW and to provide sufficient control strategies for Danish buildings using the PCM/VW ventilation system.

The numerical model built in EnergyPlus is validated by a full-scale experiment conducted in 3 parts: Summer night cooling application, winter solar energy storage application and blinds with advanced VW control including natural ventilation for self-cooling and mechanical ventilation. The comparisons of the experiment results and simulation data show that the models fit with the experimental data in all aspects. The summer night cooling model has higher accuracy than the winter energy storage model and models with absorption/reflection blinds.

Some conclusions are drawn when comparing the PCM/VW with 2 other ventilation systems to test its thermal and energy performance. Compared to the no VW, no PCM system and the VW, no PCM system, the PCM/VW for summer night cooling application reduces the cooling energy demand by 46% and 27% respectively for room 1, and 51% and 38% respectively for room 2; for winter solar energy storage application, the PCM/VW reduces the heating energy demand by 29% and 48% respectively for room 1, and 10% and 28% respectively for room 2.

The conclusions for control strategy development under Danish weather conditions are:

The developed control strategy for summer night cooling application is to use between-glass reflection shading, ventilate directly from PCM heat exchanger to the room while applying VW self-cooling for ventilation pre-cooling mode, and heat the room with air from VW to prevent overcooling of the room. The model chose different modes based on the indoor temperature sensor. Compared to the primitive strategy, the developed control strategy saves 62.3% of the energy for the room with windows facing southwest, and 58.2% of the energy for the room with windows facing northeast.

The developed control strategy for winter solar energy storage application is to use between-glass absorption blind, make use of

the hot air in VW, and to cool the VW by self-cooling and bypass ventilation to prevent the overheating of the room. Compared to the primitive strategy, the developed control strategy saves 9.4% of the energy for the room with windows facing southwest, and 4.4% of the energy for the room with windows facing northeast.

The orientations of the windows have no influence on the results of the developed control strategy. However, it has a big influence on the room's energy demand. The room with southwest facing windows has higher energy savings compared to the room with northeast facing windows. Moreover, the control strategy development of summer night cooling application has more improvement in energy efficiency than winter solar energy storage application. However, the energy demands among different control strategies have no significant differences except for the primitive control strategy for summer night cooling application. In general, the energy saving potential of PCM/VW is robust regardless of the control strategies, especially for winter solar energy storage application.

Declaration of competing interest

None.

CRediT authorship contribution statement

Yue Hu: Data curation, Investigation, Methodology, Writing - original draft, Writing - review & editing. **Rui Guo:** Visualization, Writing - original draft, Writing - review & editing. **Per Kvols Heiselberg:** Funding acquisition, Supervision, Writing - review & editing.

Acknowledgment

The EU Horizon 2020 research and innovation program under grant agreement NO. 768576(ReCO2ST) supported this work.

References

- [1] N. Soares, J.J. Costa, A.R.R. Gaspar, P. Santos, Review of Passive PCM Latent Heat Thermal Energy Storage Systems towards Buildings' Energy Efficiency, Elsevier, 2013, <https://doi.org/10.1016/j.enbuild.2012.12.042>.
- [2] M. Pomianowski, P. Heiselberg, Y. Zhang, Review of thermal energy storage technologies based on PCM application in buildings, Energy Build. 67 (2013) 56–69, <https://doi.org/10.1016/j.enbuild.2013.08.006>.
- [3] F. Kuznik, J. Virgone, K. Johannes, In-situ study of thermal comfort enhancement in a renovated building equipped with phase change material wallboard, Renew. Energy 36 (2011) 1458–1462, <https://doi.org/10.1016/j.renene.2010.11.008>.
- [4] Y. Zhang, K. Lin, Y. Jiang, G. Zhou, Thermal storage and nonlinear heat-transfer characteristics of PCM wallboard, Energy Build. 40 (2008) 1771–1779, <https://doi.org/10.1016/j.enbuild.2008.03.005>.
- [5] H. Liu, H.B. Awbi, Performance of phase change material boards under natural

- convection, *Build. Environ.* 44 (2009) 1788–1793, <https://doi.org/10.1016/j.buildenv.2008.12.002>.
- [6] P.K.S. Rathore, S.K. Shukla, An experimental evaluation of thermal behavior of the building envelope using microencapsulated PCM for energy savings, *Renew. Energy* 149 (2020) 1300–1313, <https://doi.org/10.1016/j.renene.2019.10.130>.
- [7] H. Wang, W. Lu, Z. Wu, G. Zhang, Parametric analysis of applying PCM wall-boards for energy saving in high-rise lightweight buildings in Shanghai, *Renew. Energy* 145 (2020) 52–64, <https://doi.org/10.1016/j.renene.2019.05.124>.
- [8] J. Yu, Q. Yang, H. Ye, Y. Luo, J. Huang, X. Xu, W. Gang, J. Wang, Thermal performance evaluation and optimal design of building roof with outer-layer shape-stabilized PCM, *Renew. Energy* 145 (2020) 2538–2549, <https://doi.org/10.1016/j.renene.2019.08.026>.
- [9] M. Pomianowski, P. Heiselberg, R.L. Jensen, R. Cheng, Y. Zhang, A new experimental method to determine specific heat capacity of inhomogeneous concrete material with incorporated microencapsulated-PCM, *Cement Concr. Res.* 55 (2014) 22–34, <https://doi.org/10.1016/j.cemconres.2013.09.012>. <http://linkinghub.elsevier.com/retrieve/pii/S0008884613001981>. (Accessed 2 May 2018).
- [10] R. Cheng, M. Pomianowski, X. Wang, P. Heiselberg, Y. Zhang, A new method to determine thermophysical properties of PCM-concrete brick, *Appl. Energy* 112 (2013) 988–998, <https://doi.org/10.1016/j.apenergy.2013.01.046>.
- [11] M. Pomianowski, P. Heiselberg, R.L. Jensen, R. Lund Jensen, Dynamic heat storage and cooling capacity of a concrete deck with PCM and thermally activated building system, *Energy Build.* 53 (2012) 96–107, <https://doi.org/10.1016/j.enbuild.2012.07.007>.
- [12] K.A.R. Ismail, J.R. Henriques, Parametric study on composite and PCM glass systems, *Energy Convers. Manag.* 43 (2002) 973–993, [https://doi.org/10.1016/S0196-8904\(01\)00083-8](https://doi.org/10.1016/S0196-8904(01)00083-8).
- [13] K.A.R. Ismail, C.T. Salinas, J.R. Henriques, Comparison between PCM filled glass windows and absorbing gas filled windows, *Energy Build.* 40 (2008) 710–719, <https://doi.org/10.1016/j.enbuild.2007.05.005>.
- [14] H. Weinlaeder, W. Koerner, M. Heidenfelder, Monitoring results of an interior sun protection system with integrated latent heat storage, *Energy Build.* 43 (2011) 2468–2475, <https://doi.org/10.1016/j.enbuild.2011.06.007>.
- [15] H. Johra, P. Heiselberg, Influence of internal thermal mass on the indoor thermal dynamics and integration of phase change materials in furniture for building energy storage: a review, *Renew. Sustain. Energy Rev.* 69 (2017) 19–32, <https://doi.org/10.1016/j.rser.2016.11.145>.
- [16] H. Johra, P. Heiselberg, J. Le Dréau, Influence of envelope, structural thermal mass and indoor content on the building heating energy flexibility, *Energy Build.* 183 (2019) 325–339, <https://doi.org/10.1016/j.enbuild.2018.11.012>.
- [17] H. Weinlaeder, W. Korner, B. Strieder, A ventilated cooling ceiling with integrated latent heat storage-Monitoring results, *Energy Build.* 82 (2014) 65–72, <https://doi.org/10.1016/j.enbuild.2014.07.013>.
- [18] R. Ansuini, R. Larchetti, A. Giretti, M. Lemma, Radiant floors integrated with PCM for indoor temperature control, *Energy Build.* 43 (2011) 3019–3026, <https://doi.org/10.1016/j.enbuild.2011.07.018>.
- [19] X. Jin, X. Zhang, Thermal analysis of a double layer phase change material floor, *Appl. Therm. Eng.* 31 (2011) 1576–1581, <https://doi.org/10.1016/j.applthermaleng.2011.01.023>.
- [20] A. De Gracia, L. Navarro, A. Castell, L.F. Cabeza, L.F. Cabeza, Numerical study on the thermal performance of a ventilated facade with PCM, *Appl. Therm. Eng.* 61 (2013) 372–380, <https://doi.org/10.1016/j.applthermaleng.2013.07.035>.
- [21] Y. Hu, P. Heiselberg, A new ventilated window with PCM heat exchanger – performance analysis and design optimization, *Energy Build.* 169 (2018) 185–194, <https://doi.org/10.1016/j.enbuild.2018.03.060>.
- [22] F. Motte, G. Notton, C. Lamnatou, C. Cristofari, D. Chemisana, Numerical study of PCM integration impact on overall performances of a highly building-integrated solar collector, *Renew. Energy* 137 (2019) 10–19, <https://doi.org/10.1016/j.renene.2017.12.067>.
- [23] J.R. Turnpenny, D.W. Etheridge, D.A. Reay, Novel ventilation cooling system for reducing air conditioning in buildings: Part I: testing and theoretical modelling, *Appl. Therm. Eng.* 20 (2000) 1019–1037, [https://doi.org/10.1016/S1359-4311\(99\)00068-X](https://doi.org/10.1016/S1359-4311(99)00068-X).
- [24] D.J. Morrison, S.I. Abdel-Khalik, Effects of phase-change energy storage on the performance of air-based and liquid-based solar heating systems, *Sol. Energy* 20 (1978) 57–67, [https://doi.org/10.1016/0038-092X\(78\)90141-X](https://doi.org/10.1016/0038-092X(78)90141-X).
- [25] S. Canbazoglu, A.S. Sahinaslan, A. Ekmekyapar, Y. Gökhan Aksoy, F. Akarsu, Enhancement of solar thermal energy storage performance using sodium thiosulfate pentahydrate of a conventional solar water-heating system, *Energy Build.* 37 (2005) 235–242, <https://doi.org/10.1016/j.enbuild.2004.06.016>.
- [26] M.J. Huang, P.C. Eames, S. McCormack, P. Griffiths, N.J. Hewitt, Micro-encapsulated phase change slurries for thermal energy storage in a residential solar energy system, *Renew. Energy* 36 (2011) 2932–2939, <https://doi.org/10.1016/j.renene.2011.04.004>.
- [27] D. Appelfeld, C.S. Hansen, S. Svendsen, Development of a slim window frame made of glass fibre reinforced polyester, *Energy Build.* (2010), <https://doi.org/10.1016/j.enbuild.2010.05.028>.
- [28] M. Liu, P.K. Heiselberg, O.K. Larsen, L. Mortensen, J. Rose, Investigation of different configurations of a ventilated window to optimize both energy efficiency and thermal comfort, *Energy Procedia* 132 (2017) 478–483, <https://doi.org/10.1016/j.egypro.2017.09.660>.
- [29] J. Tanimoto, K.I. Kimura, Simulation study on an air flow window system with an integrated roll screen, *Energy Build.* 26 (1997) 317–325, [https://doi.org/10.1016/S0378-7788\(97\)00012-1](https://doi.org/10.1016/S0378-7788(97)00012-1).
- [30] J. Wei, J. Zhao, Q. Chen, Optimal design for a dual-airflow window for different climate regions in China, *Energy Build.* 42 (2010) 2200–2205, <https://doi.org/10.1016/j.enbuild.2010.07.016>.
- [31] T. tai Chow, Z. Lin, K. fai Fong, L. shun Chan, M. miao He, Thermal performance of a natural airflow window in subtropical and temperate climate zones - a comparative study, *Energy Convers. Manag.* 50 (2009) 1884–1890, <https://doi.org/10.1016/j.enconman.2009.04.028>.
- [32] D. Appelfeld, S. Svendsen, Experimental analysis of energy performance of a ventilated window for heat recovery under controlled conditions, *Energy Build.* 43 (2011) 3200–3207, <https://doi.org/10.1016/j.enbuild.2011.08.018>.
- [33] J.S. Carlos, H. Corvacho, Evaluation of the performance indices of a ventilated double window through experimental and analytical procedures: SHGC-values, *Energy Build.* 86 (2015) 886–897, <https://doi.org/10.1016/j.enbuild.2014.11.002>.
- [34] J.S. Carlos, Optimizing the ventilated double window for solar collection, *Sol. Energy* 150 (2017) 454–462, <https://doi.org/10.1016/j.solener.2017.04.063>.
- [35] J.S. Carlos, H. Corvacho, P.D. Silva, J.P. Castro-Gomes, Real climate experimental study of two double window systems with preheating of ventilation air, *Energy Build.* 42 (2010) 928–934, <https://doi.org/10.1016/j.enbuild.2010.01.003>. <https://www.sciencedirect.com/science/article/pii/S0378778810000095>. (Accessed 21 August 2019).
- [36] Y. Hu, P. Heiselberg, R. Guo, Ventilation cooling/heating performance of a PCM enhanced ventilated window - an experimental study, *Energy Build.* (2020) 109903, <https://doi.org/10.1016/j.enbuild.2020.109903>. Accepted.
- [37] P.G. Schild, M. Mysen, Technical note AIVC 65: recommendations on specific fan power and fan system efficiency. <https://www.aivc.org/resource/tn-65-recommendations-specific-fan-power-and-fan-system-efficiency>, 2009. (Accessed 28 November 2019).
- [38] Y. Hu, P. Heiselberg, H. Johra, R. Guo, Experimental and numerical study of a PCM solar air heat exchanger and its ventilation preheating effectiveness, *Renew. Energy* 145 (2019) 106–115, <https://doi.org/10.1016/j.renene.2019.05.115>.
- [39] Kim Bjarne Wittchen, Vurdering af potentialet for varmebesparelser i eksisterende boliger. <https://sbi.dk/Pages/Vurdering-af-potentialet-for-varmebesparelser-i-eksisterende-boliger.aspx>, 2004. (Accessed 3 April 2019).
- [40] R. Jensen, J. Nørgaard, O. Daniels, R. Justesen, Person- Og Forbrugsprofiler: Bygningsintegreret Energiforsyning, 2011.